Electronic Supplementary Material (ESI) for New Journal of Chemistry.

Complexes of phosphonate and phosphinate derivatives of dipicolylamine

Veronika Hlinová, Adam Jaroš, Tomáš David, Ivana Císařová, Jan Kotek, Vojtěch Kubíček,* Petr Hermann

Department of Inorganic Chemistry, Faculty of Science, Charles University, Hlavova 2030, 128 40 Prague, Czech Republic. E-mail: kubicek@natur.cuni.cz; Tel.: +420 221951436; Fax: +420 221921253.

Table of contents

Figure S1. Characterization $^{31}P\{^{1}H\}$ (**A**), ^{1}H (**B**) and $^{13}C\{^{1}H\}$ (**C**) NMR spectra of $H_2\mathbf{L^1}$ (≥99% purity) in D_2O (pD ~ 5) accompanied with HPLC trace (**D**; *M1*; 254 nm black, 280 nm cyan).

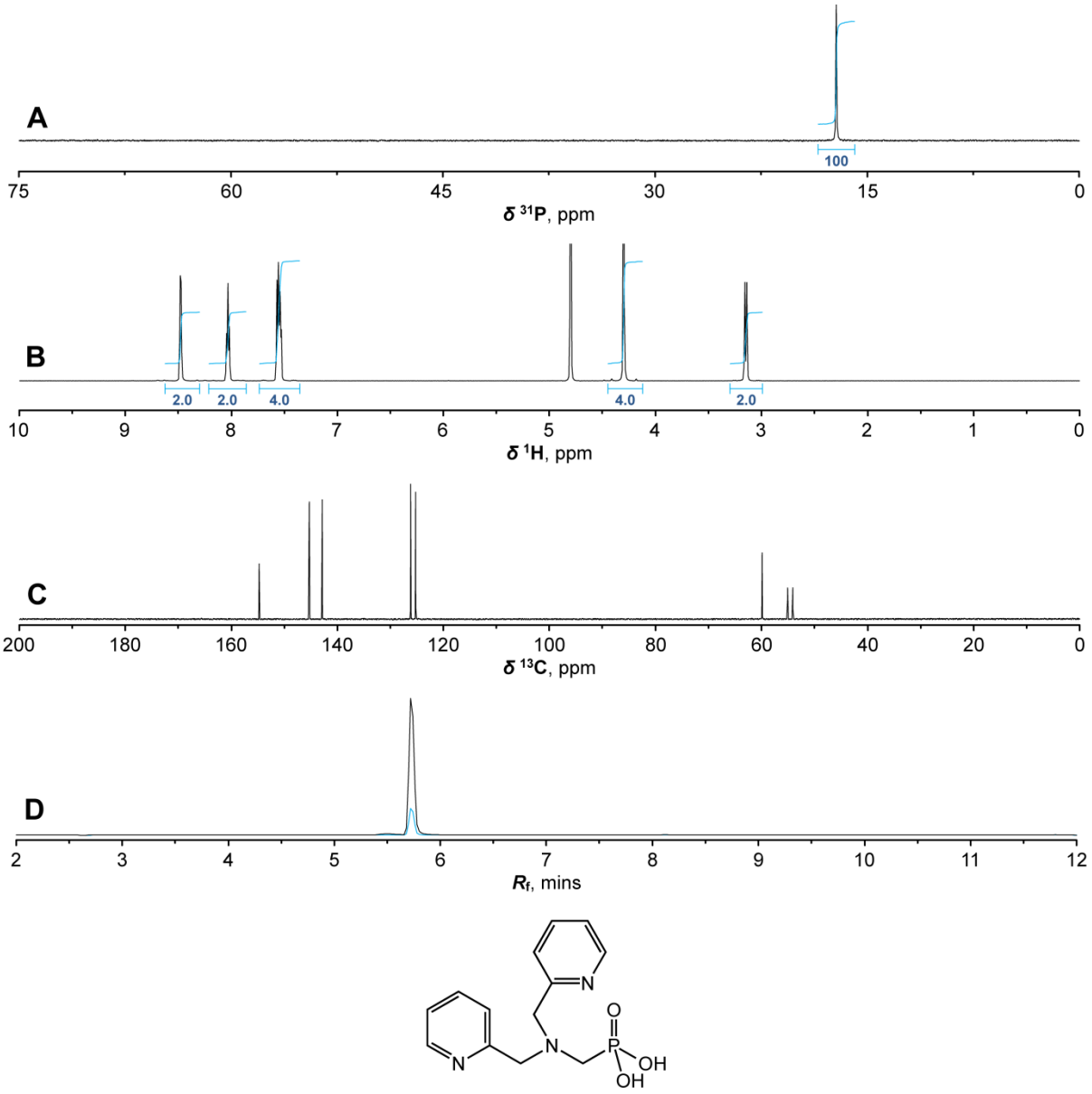

Figure S2. Characterization ^{31}P (**A**), ^{1}H (**B**) and $^{13}C\{^{1}H\}$ (**C**) NMR spectra of H**L**^{2} (~98% purity) in D_2O (pD ~ 5) accompanied with HPLC trace (**D**; *M1*; 254 nm black, 280 nm cyan).

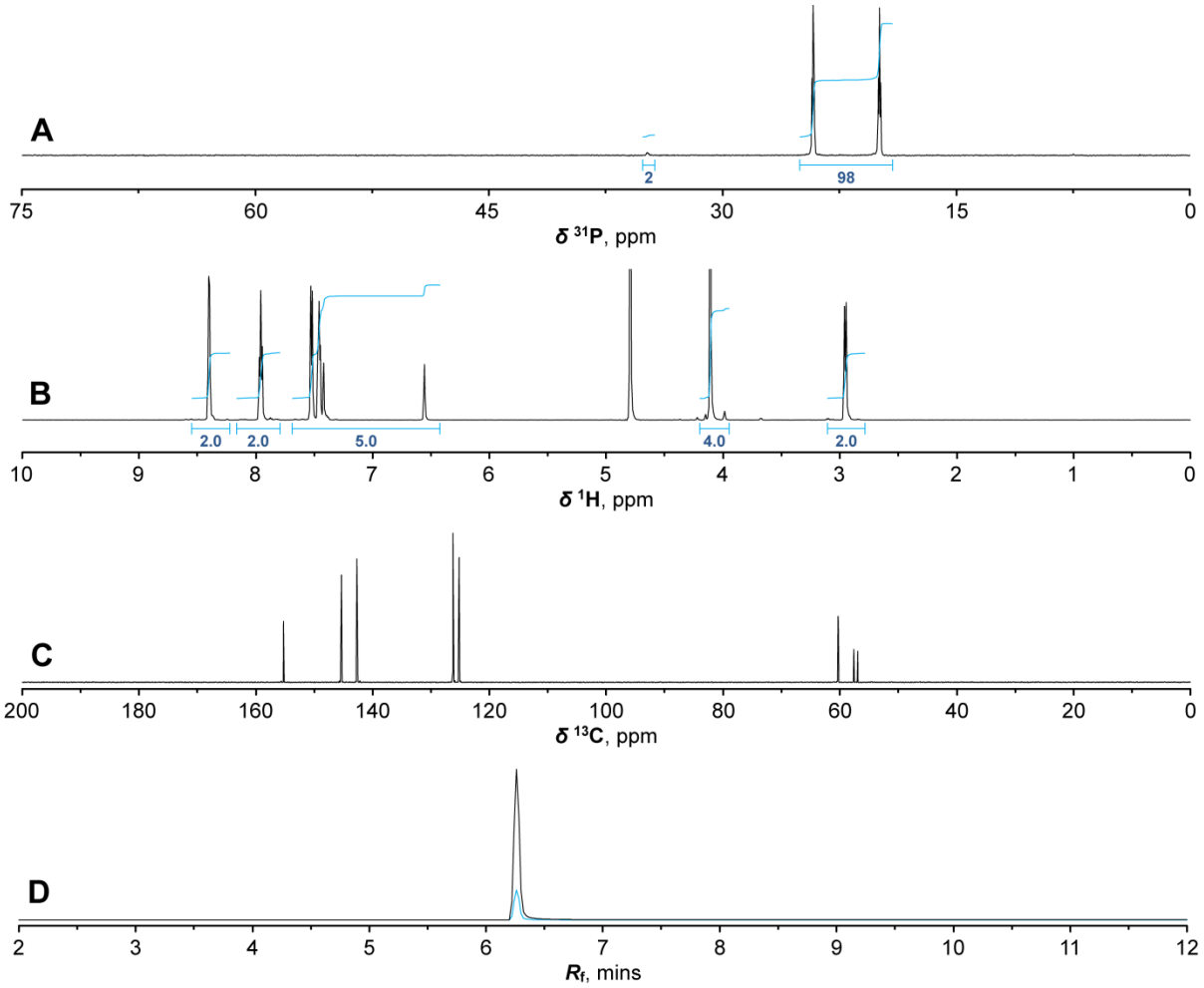

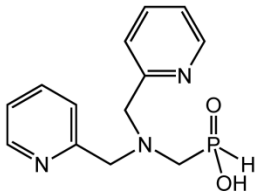

Figure S3. Characterization $^{31}P\{^{1}H\}$ (**A**), ^{1}H (**B**) and $^{13}C\{^{1}H\}$ (**C**) NMR spectra of H**L**^{3} (~96% purity) in D_2O (pD ~ 4) accompanied with HPLC trace (**D**; *M1*; 254 nm black, 280 nm cyan).

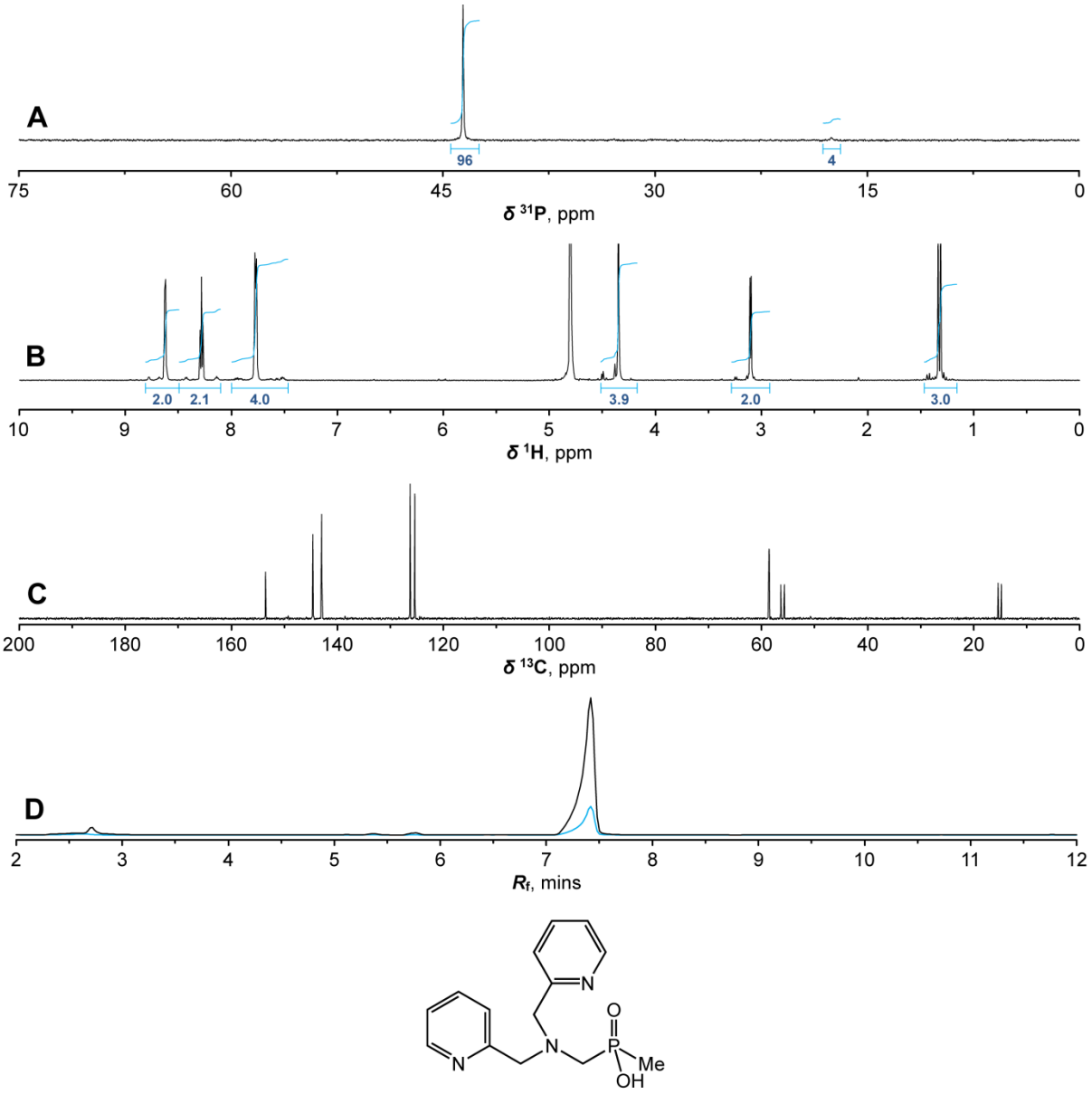

Figure S4. Characterization ^{31}P (**A**), ^{1}H (**B**) and $^{13}C\{^{1}H\}$ (**C**) NMR spectra of $H_2\mathbf{L}^{\mathbf{4}}$ (~98% purity) in D_2O (pD ~ 3) accompanied with HPLC trace (**D**; *M1*; 254 nm black, 280 nm cyan).

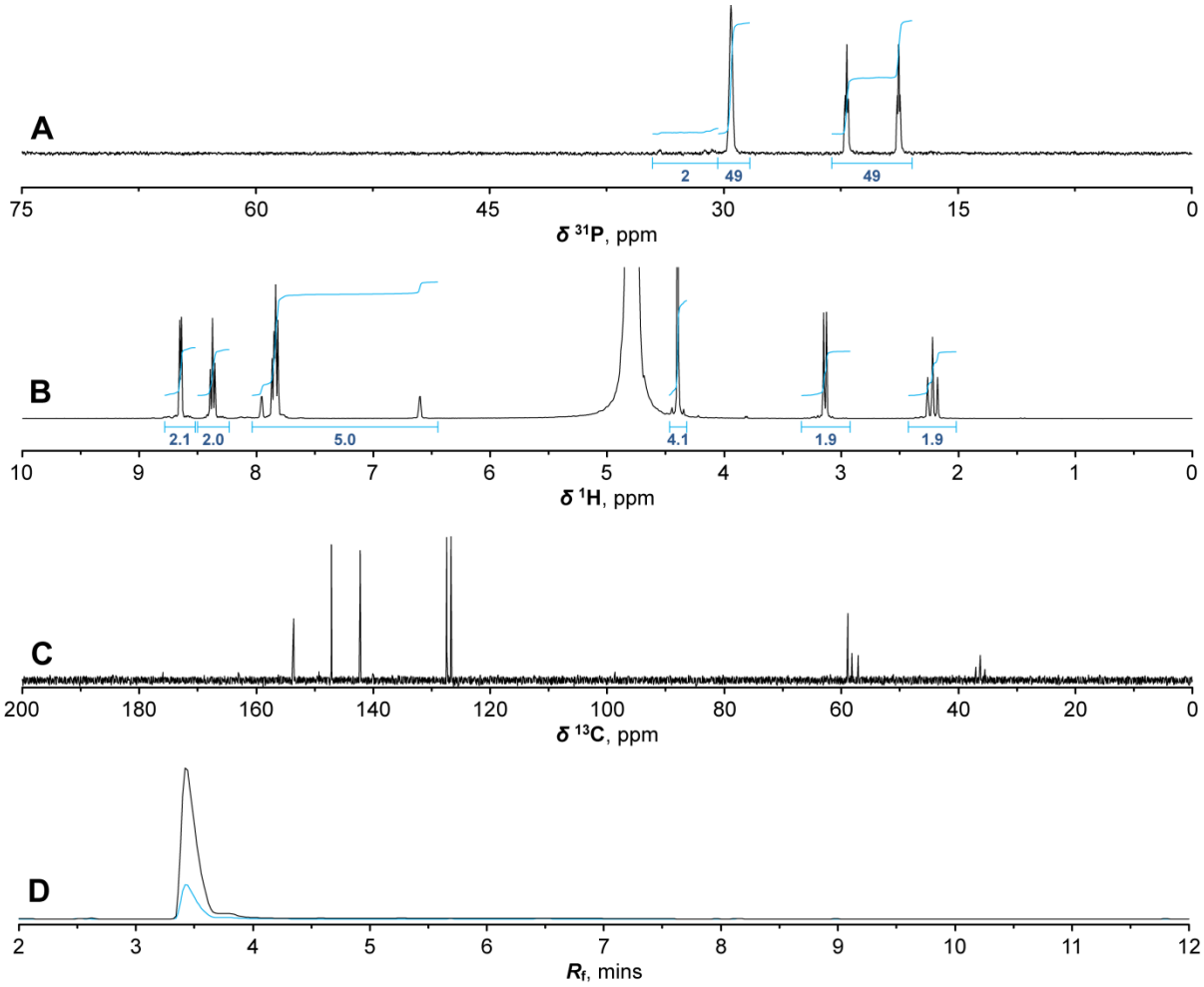

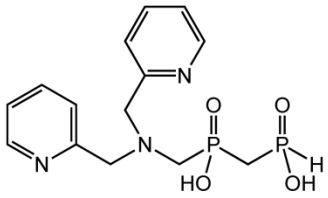

Figure S5. Characterization ^{31}P (**A**) and ^{1}H (**B**) NMR spectra of *N*,*N*,*N*',*N*'-tetrakys(2-methylpyridyl)-bis(aminomethyl)phosphinic acid (≥95% purity) in D_2O (pD ~ 5) accompanied with HPLC trace (**C**; *M1*; 254 nm black, 280 nm cyan). The compound was isolated by reverse-phase flash chromatography (C18) from a long-stored (months) oily zwitterionic form of H**L**^{2}. **Purity** (^{31}P and ^{1}H NMR): ≥95 %. **NMR** (D_2O, pD ~ 5): **^{1}H** δ 2.85 (P–CH_2–N, d, 4H, $^{2}J_{HP}$ = 9); 3.87 (CH_2–N–CH_2, s, 8H); 7.31 (*H*$_2$, ddd, 4H, $^{3}J_{HH}$ = 8, $^{3}J_{HH}$ = 5, $^{4}J_{HH}$ = 1); 7.34 (*H*$_4$, ddd, 4H, $^{3}J_{HH}$ = 8, $^{4}J_{HH}$ = 1, $^{5}J_{HH}$ = 1); 7.77 (*H*$_3$, ddd, 4H, $^{3}J_{HH}$ = 8, $^{3}J_{HH}$ = 8, $^{4}J_{HH}$ = 2); 8.33 (*H*$_1$, ddd, 4H, $^{3}J_{HH}$ = 5, $^{4}J_{HH}$ = 2, $^{5}J_{HH}$ = 1); **^{31}P**{^{1}H} δ 34.9 (s). **ESI-MS**: **(−)** 487.0 [M−H$^+$]$^-$; **(+)** 489.1 [M+H$^+$]$^+$; 511.1 [M+Na$^+$]$^+$; 527.1 [M+K$^+$]$^+$. **TLC** (EtOH – conc. aq. NH_4OH 7:1): R_f ~ 0.6. **HPLC**: R_f ~ 8.5 min.

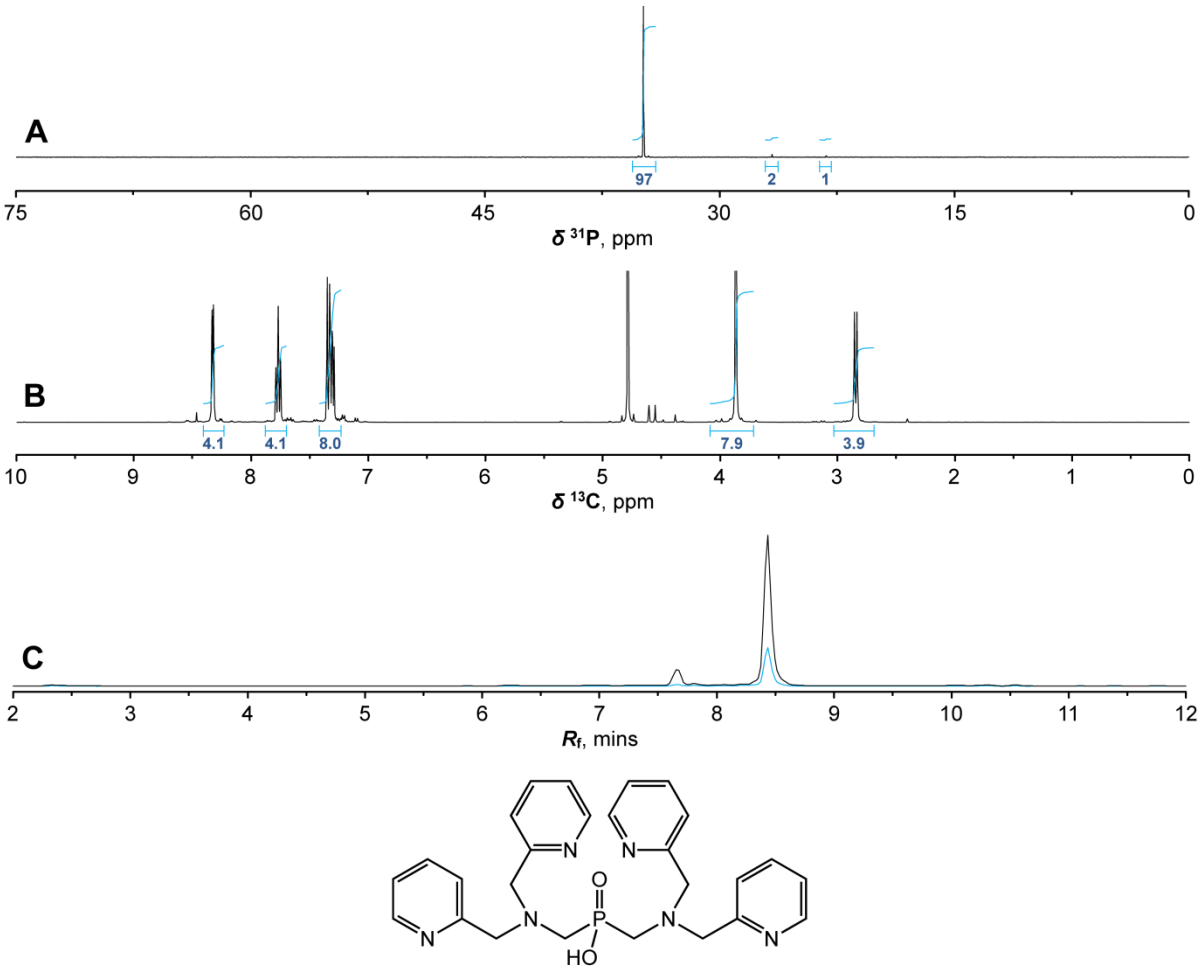

Table S1. Overall protonation constants logβ(H_nL) of the studied compounds (25 °C, I = 0.1 M (NMe_4)Cl). Charges of individual species are omitted.

	H_2**L**[1]	H**L**[2]	H**L**[3]	H_2**L**[4]
HL	8.39(1)	6.13(1)	6.38(2)	6.83(1)
H_2L	14.31(1)	10.27(1)	10.56(2)	11.55(2)
H_3L	18.43(1)	11.25(2)	11.62(3)	12.18(5)
H_4L	19.24(4)	–	–	–

Figure S6. ^{1}H NMR titration of $H_2\mathbf{L}^{1}$ (**A**, c_L ~ 50 mM, 25 °C) and $H_2\mathbf{L}^{4}$ (**B**, c_L ~ 50 mM, 25 °C). Solid lines represent the best fits. Vertical dotted grey lines indicate the potentiometrically determined consecutive protonation constants.

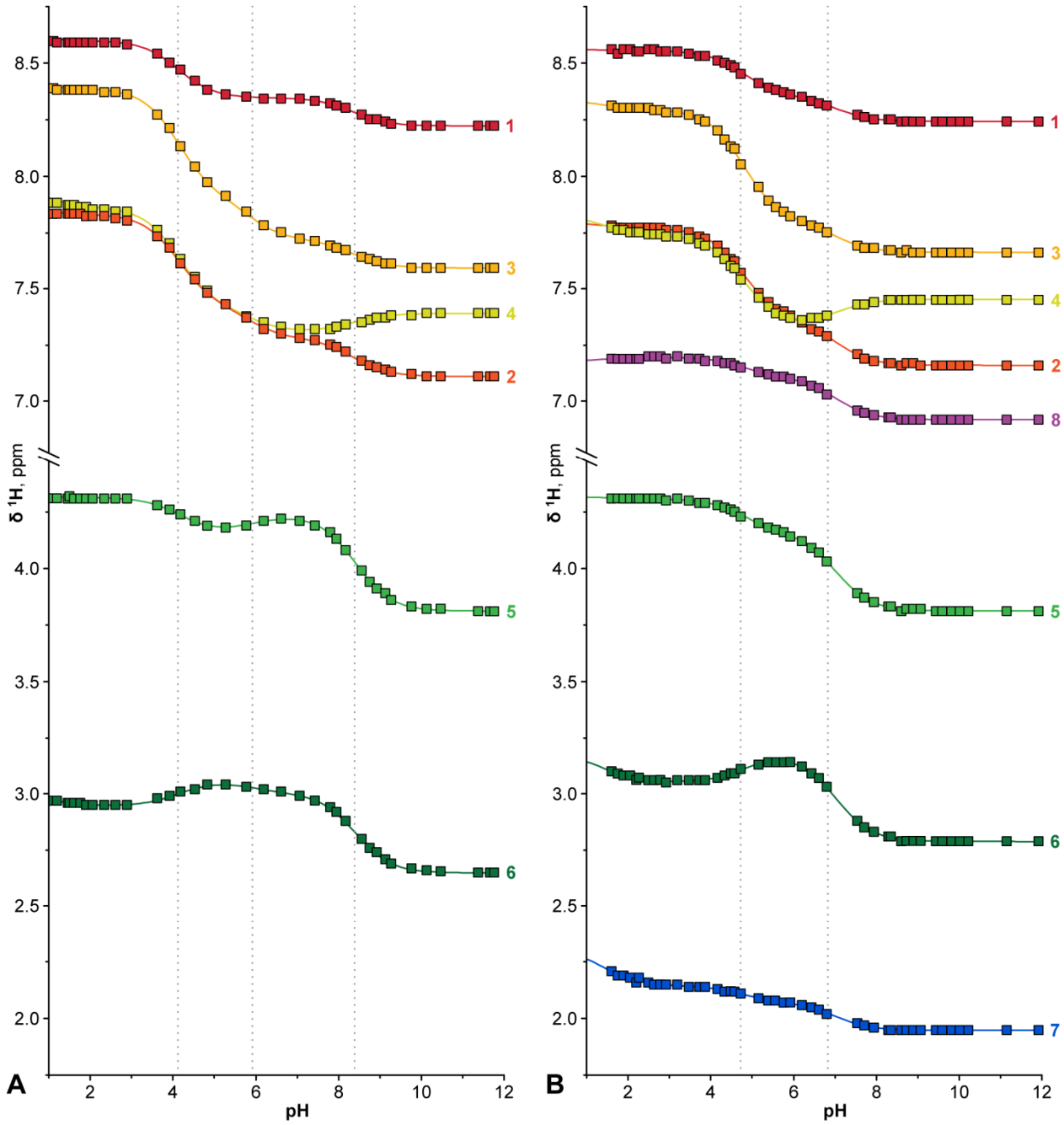

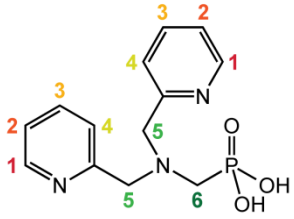

$H_2\mathbf{L}^{1}$

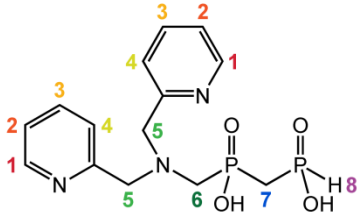

$H_2\mathbf{L}^{4}$

Figure S7. ^{13}C {^{1}H} NMR titration of $H_2\mathbf{L}^{1}$ (**A**, c_L ~ 50 mM, 25 °C) and $H_2\mathbf{L}^{4}$ (**B**, c_L ~ 50 mM, 25 °C). Solid lines represent the best fits. Vertical dotted grey lines indicate the potentiometrically determined consecutive protonation constants.

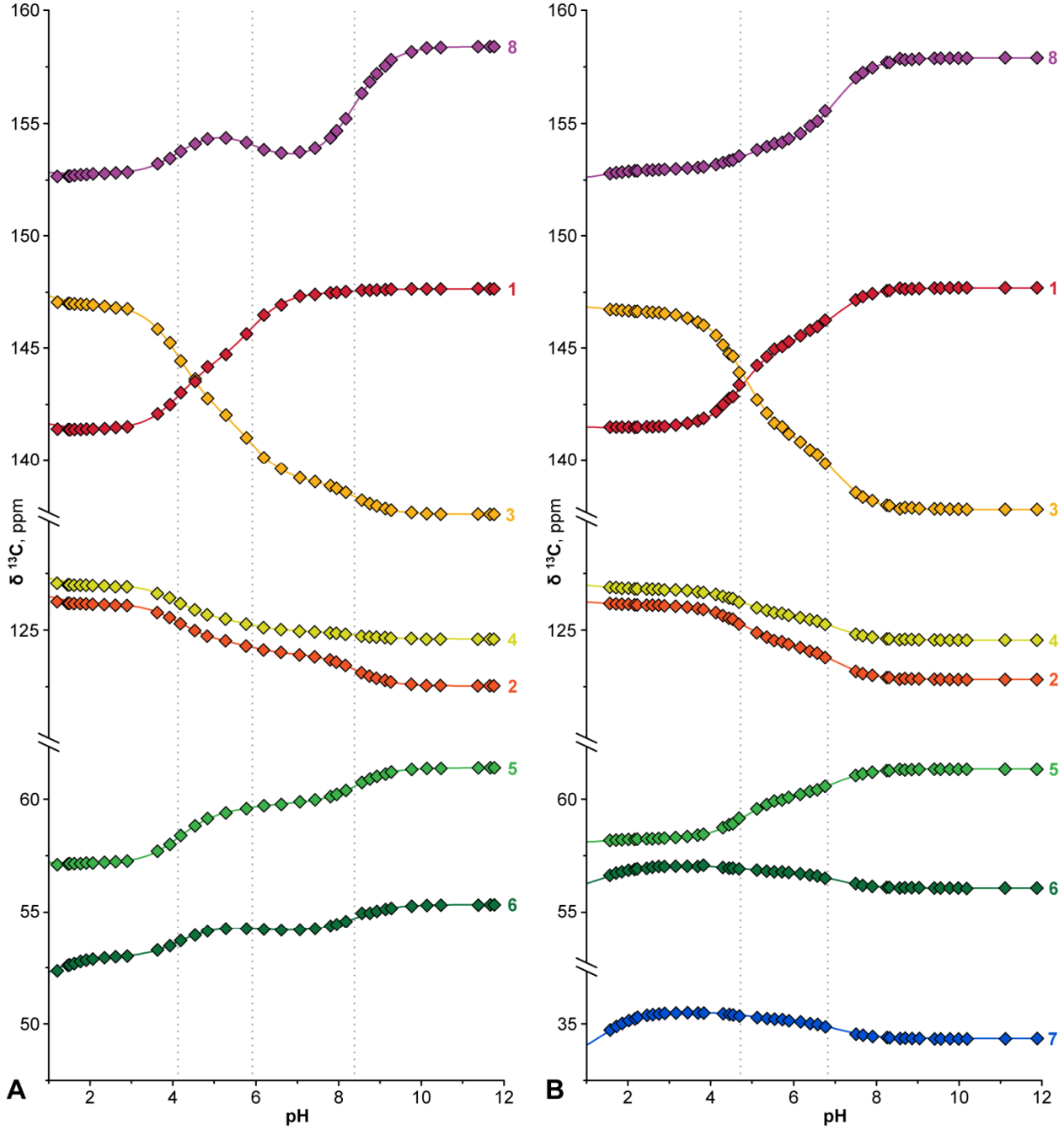

$H_2\mathbf{L}^{1}$ $H_2\mathbf{L}^{4}$

Figure S8. ^{31}P NMR titration of *P*–H (**A**) and N–CH_2–*P* (**B**) signal (the lines represent the best fits) and distribution diagram of $H_2\mathbf{L}^4$ (**C**) (c_L ~ 50 mM, 25 °C).

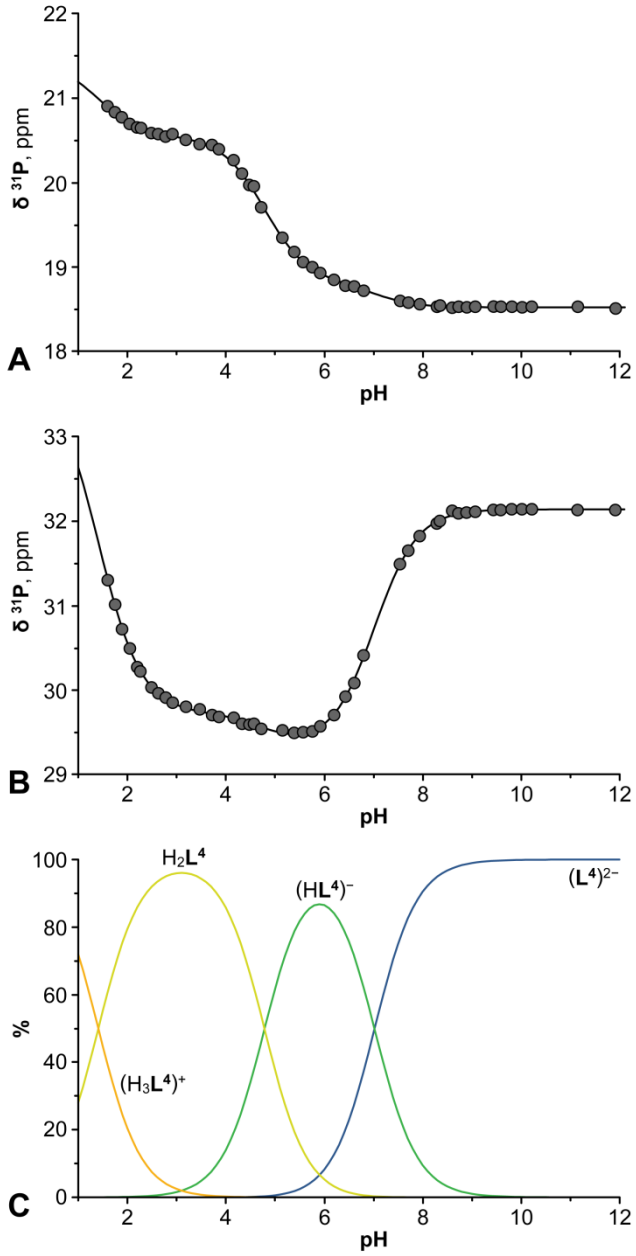

Figure S9. Suggested protonation scheme of $H_2\mathbf{L}^4$.

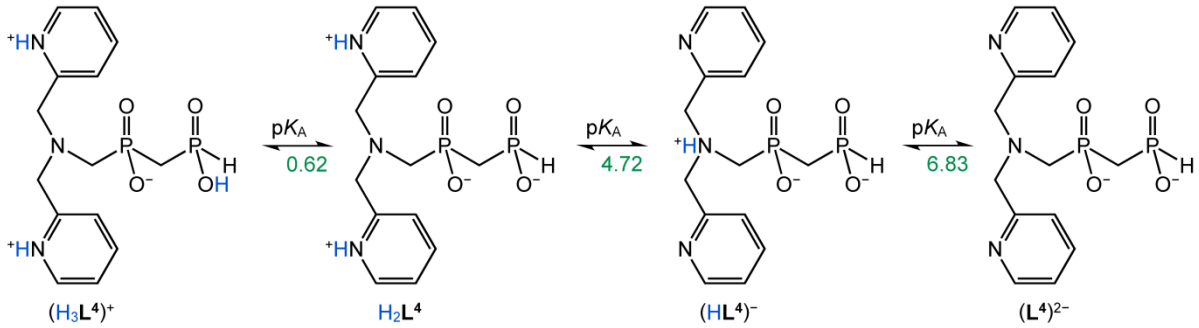

Table S2. Overall stability constants logβ of the studied complexes (25 °C, I = 0.1 M $(NMe_4)Cl$). Charges of individual species are omitted.

	H_2L^1				
	Cu(II)	**Zn(II)**	**Ni(II)**	**Mg(II)**	**Ca(II)**
[M(L)]	18.11(3)	13.26(2)	13.43(2)	4.18(4)	4.89(3)
[M(HL)]	22.73(3)	17.55(2)	18.82(2)	11.50(5)	11.43(4)
$[M(H_2L)]$	–	19.22(6)	–	16.97(4)	16.93(4)
[M(L)(OH)]	8.67(3)	3.27(3)	0.80(3)	–	–

	HL^2		
	Cu(II)	**Zn(II)**	**Ni(II)**
[M(L)]	14.64(3)	9.16(1)	10.94(2)
[M(HL)]	–	10.70(6)	–
[M(L)(OH)]	5.84(3)	–0.13(2)	–0.77(2)
$[M(L)(OH)_2]$	–	–12.61(4)	–

	HL^3		
	Cu(II)	**Zn(II)**	**Ni(II)**
[M(L)]	13.41(3)	9.61(2)	10.68(2)
[M(HL)]	14.43(2)	11.07(9)	–
[M(L)(OH)]	4.66(3)	0.40(3)	–1.06(3)
$[M(L)(OH)_2]$	–7.92(3)	–11.95(4)	–

	H_2L^4		
	Cu(II)	**Zn(II)**	**Ni(II)**
[M(L)]	13.36(5)	9.94(1)	11.78(2)
[M(HL)]	15.09(5)	–	–
[M(L)(OH)]	4.48(5)	0.53(1)	–0.14(2)
$[M(L)(OH)_2]$	–	–12.35(3)	–

Table S3. Phosphonate and phosphinate analogues of glycine: the first protonation constants and stability constants of [CuL] and [NiL] species.[1,2]

	pK_1	logK_{CuL}	logK_{NiL}
H_2GlyP	10.04	8.10	5.30
$HGlyP^{tBu}$	8.43	5.35	3.65
$HGlyP^{Me}$	8.4	4.6	3.24
$HGlyP^{Ph}$	8.08	4.41	2.91
$HGlyP^{H}$	8.07	4.84	3.60

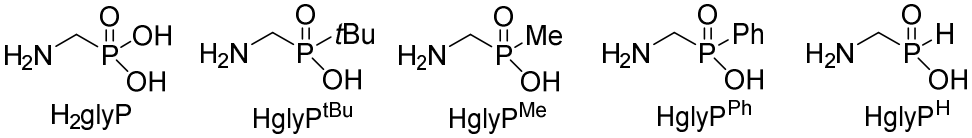

Figure S10. Distribution diagrams of Ni(II)–H_2**L**^{1} (**A**) and Mg(II)–H_2**L**^{1} (**B**) systems (c_M = c_L = 4 mM, 25 °C, I = 0.1 M $(NMe_4)Cl$).

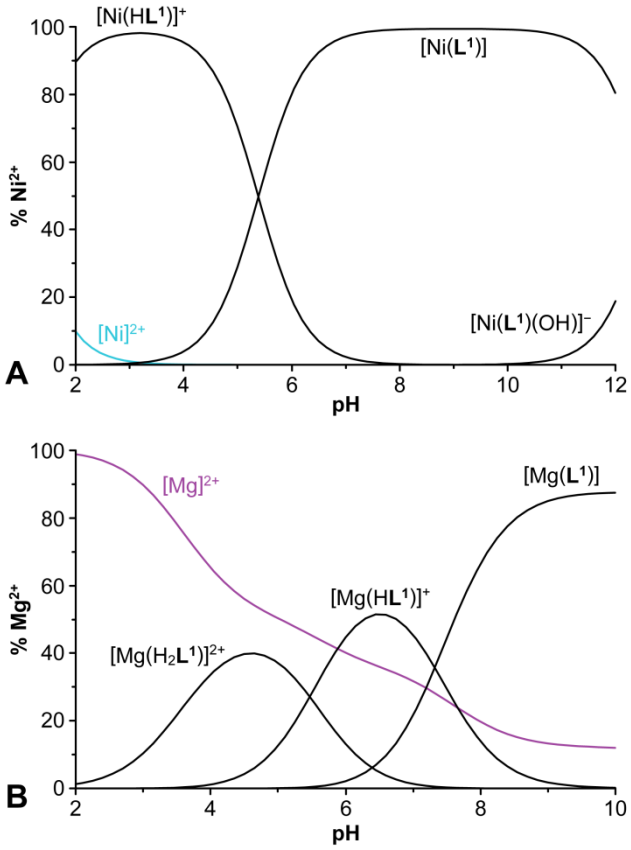

Figure S11. Distribution diagrams of Cu(II)–H**L**^{2} (**A**), Zn(II)–H**L**^{2} (**B**) and Ni(II)–H**L**^{2} (**C**) systems (c_M = c_L = 4 mM, 25 °C, I = 0.1 M (NMe_4)Cl).

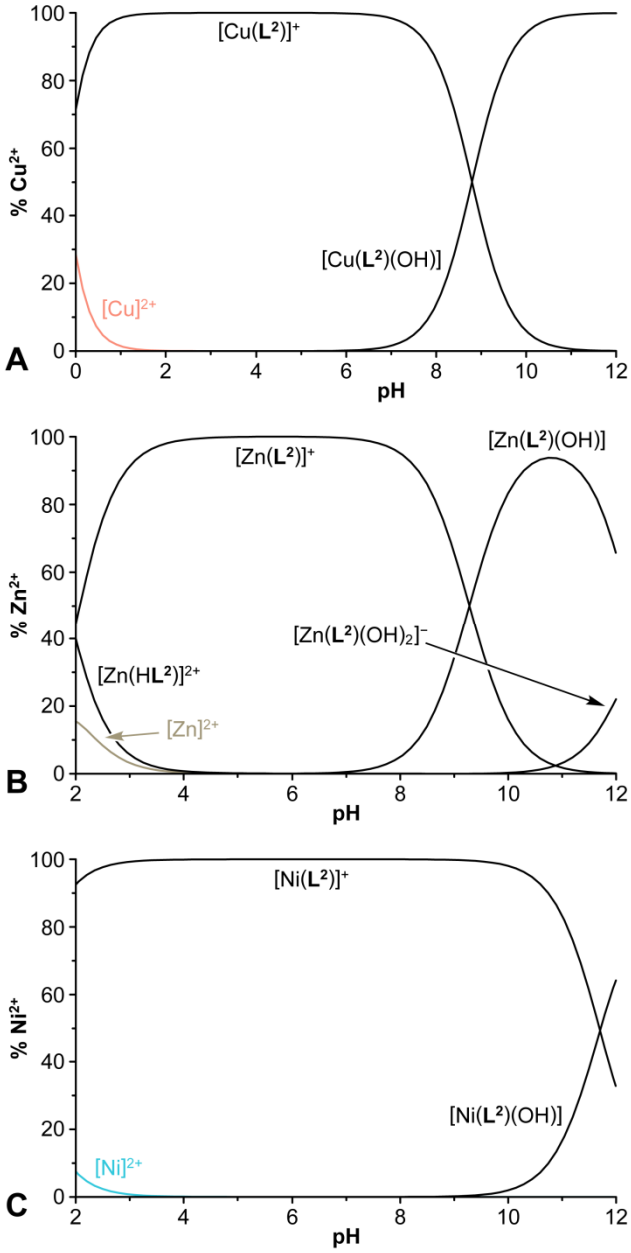

Figure S12. Distribution diagrams of Cu(II)–H**L**^{3} (**A**), Zn(II)–H**L**^{3} (**B**) and Ni(II)–H**L**^{3} (**C**) systems (c_M = c_L = 4 mM, 25 °C, I = 0.1 M (NMe_4)Cl).

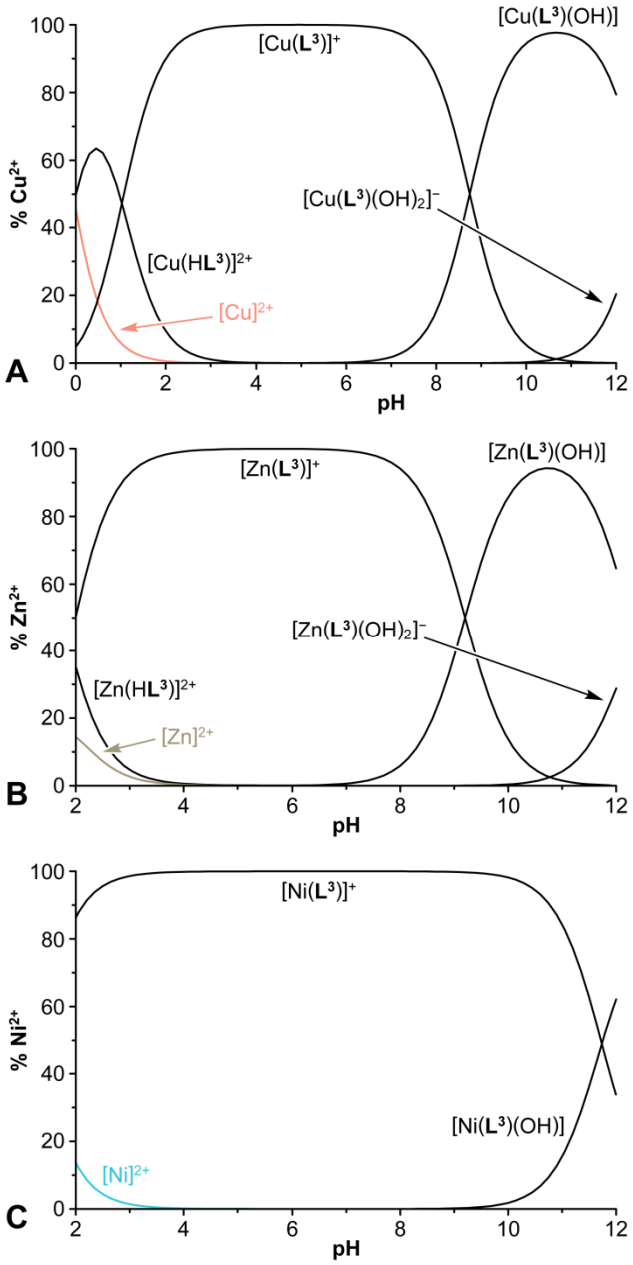

Figure S13. Distribution diagrams of Zn(II)–H_2**L**^{4} (**A**) and Ni(II)–H_2**L**^{4} (**B**) systems (c_M = c_L = 4 mM, 25 °C, I = 0.1 M (NMe_4)Cl).

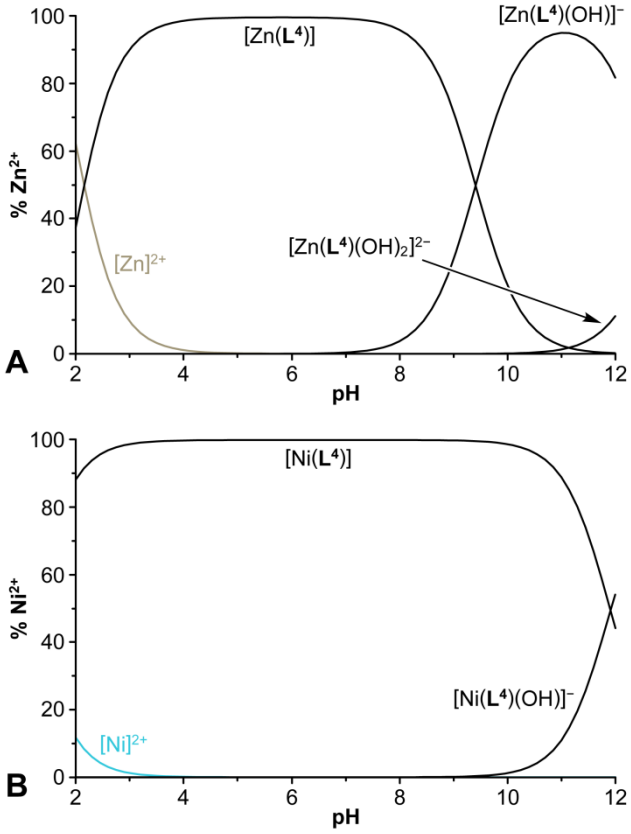

Figure S14. UV-VIS titrations of Cu(II) systems with $H_2\mathbf{L}^1$ (**A**), $H\mathbf{L}^2$ (**B**), $H\mathbf{L}^3$ (**C**) and $H_2\mathbf{L}^4$ (**D**). Spectral changes (left) and changes of absorbance at maximum of the complex absorption band (right) ($c_{Cu} = c_L$ = 4 mM, 25 °C) are shown. The solid lines represent the best fits.

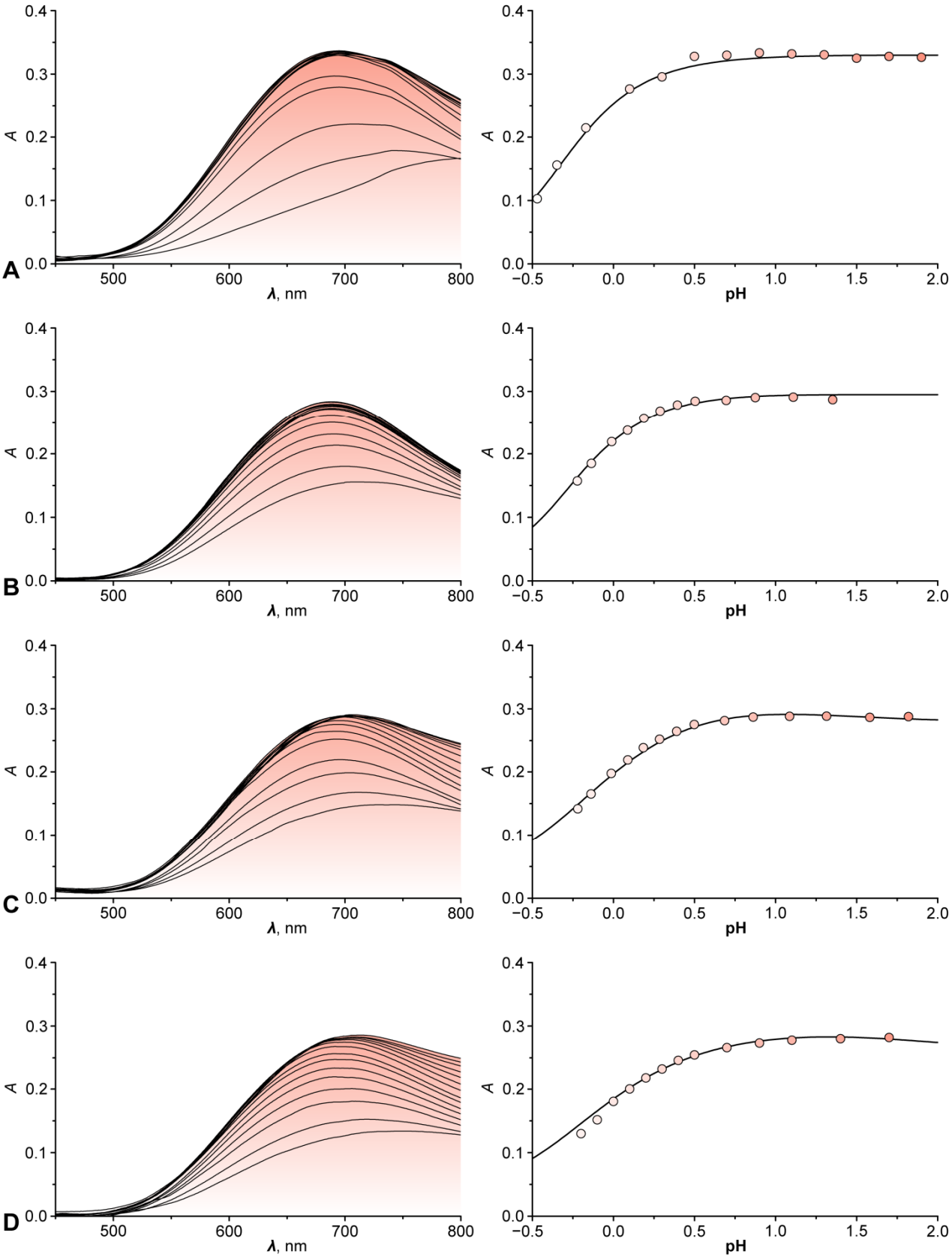

Table S4. Coordination geometry of Li(I) ion found in the crystal structure of {[Li(H$\mathbf{L}^{1}$)]$_2$}.

	distances (Å)
Li1–N1	2.313(4)
Li1–N12	2.096(4)
Li1–N22	2.130(4)
Li1–O31	2.025(4)
Li1–O31$^{\#}$	1.922(4)

$^{\#}$ symmetry-related atom (–*x*+1,–*y*+1,–*z*+1)

	angles (°)
N1–Li1–N12	77.4(1)
N1–Li1–N22	75.7(1)
N1–Li1–O31	84.3(1)
N1–Li1–O31$^{\#}$	175.3(2)
N12–Li1–N22	109.9(2)
N12–Li1–O31	112.5(2)
N12–Li1–O31$^{\#}$	105.6(2)
N22–Li1–O31	127.2(2)
N22–Li1–O31$^{\#}$	106.2(2)
O31–Li1–O31$^{\#}$	91.2(2)

$^{\#}$ symmetry-related atom (–*x*+1,–*y*+1,–*z*+1)

Figure S15. Dimeric unit {[Li(H**L**^{1})]$_2$} found in its crystal structure. Carbon-bound hydrogen atoms are not shown.

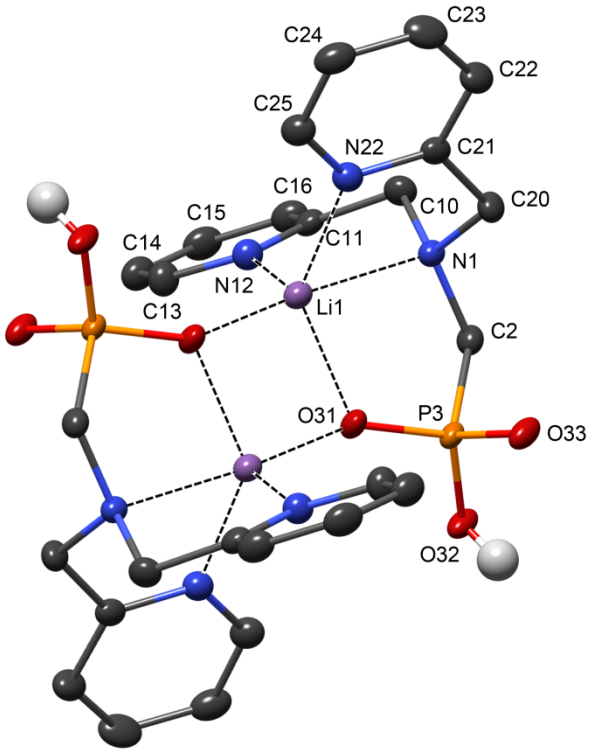

Figure S16. Crystal packing found in the crystal structure of [CuCl(H**L**^{1})]·3H_2O. Formation of eight-membered ring closed by two short hydrogen bonds between monoprotonated phosphonate groups and centrosymmetric bottom-to-bottom orientation of square bases of neighbouring complex molecules are shown. Water molecules of crystallization and carbon-bound hydrogen atoms are not shown.

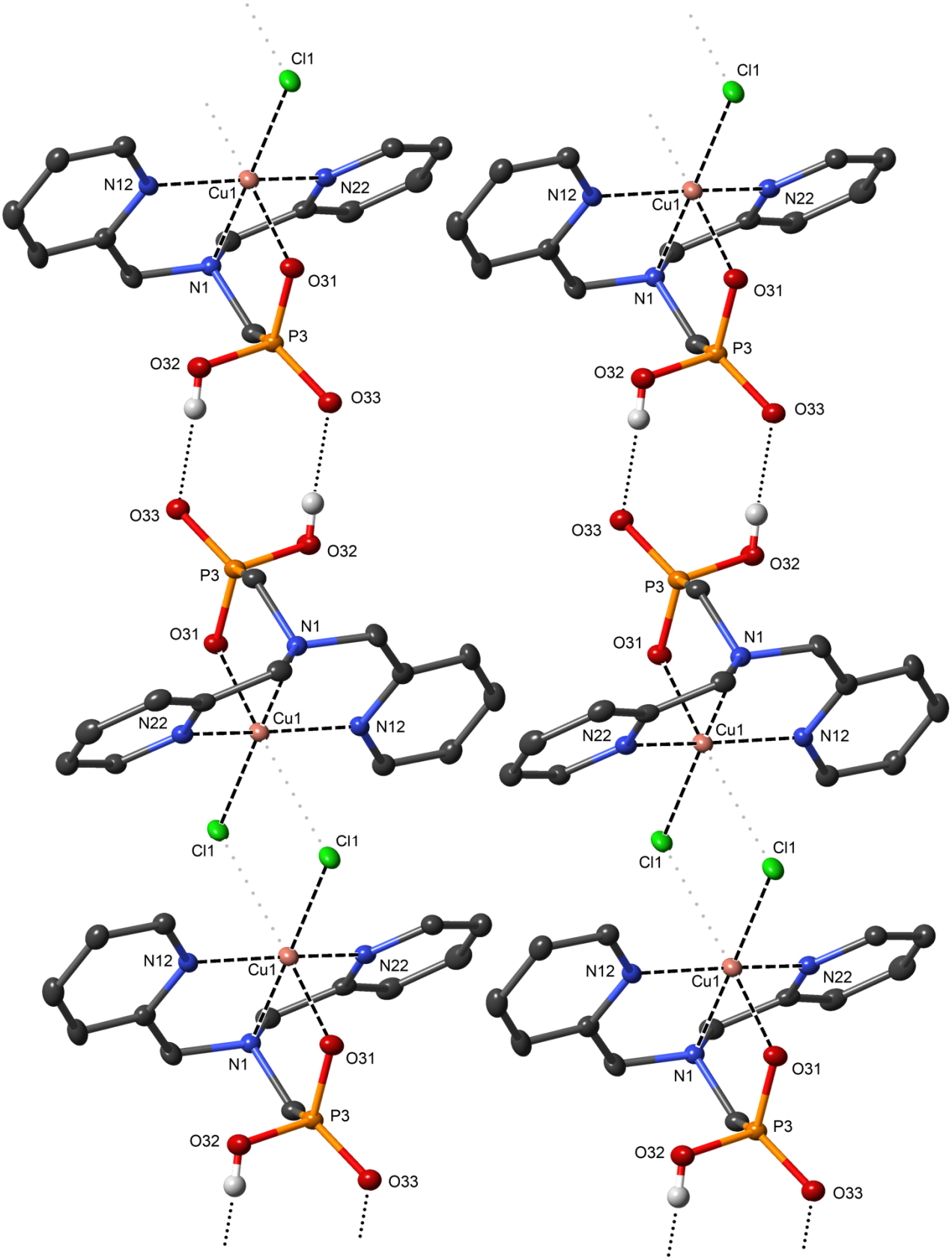

Figure 17. Crystal packing found in the crystal structure of [Cu(Cl)(H**L**^{1})] showing an intermolecular coordination of oxygen atom in apical position of the neighbouring complex. Carbon-bound hydrogen atoms are not shown.

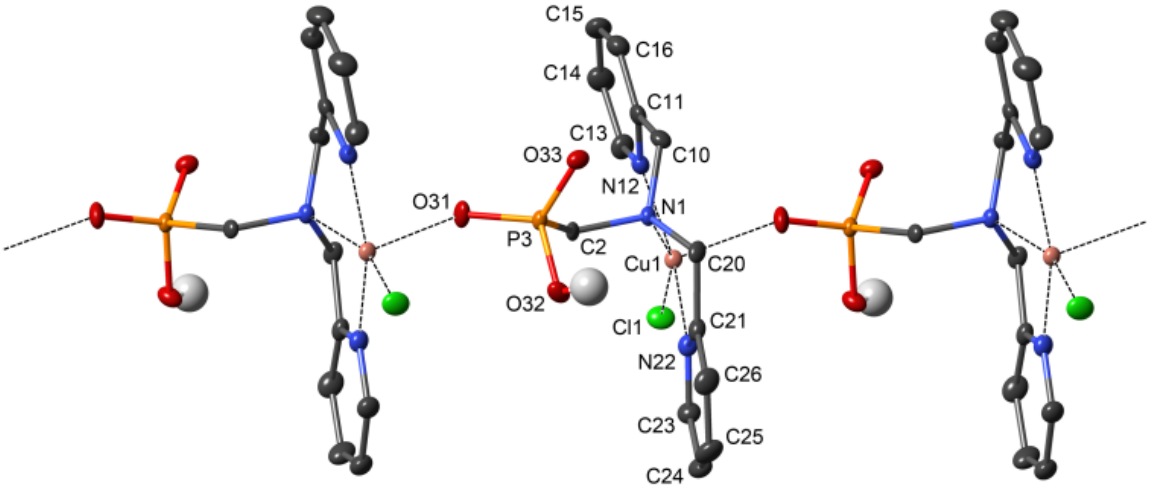

Figure S18. [CuCl(H$_2$**L**^{1})]$^{+}$ and [CuCl(H**L**^{1})] units found in the crystal structure of [CuCl(H$_2$**L**^{1})][CuCl(H**L**^{1})]Cl·H$_2$O; mutual bottom-to-bottom orientation of the complexes is shown. Water molecule of crystallization, non-coordinated chloride anion and carbon-bound hydrogen atoms are not shown.

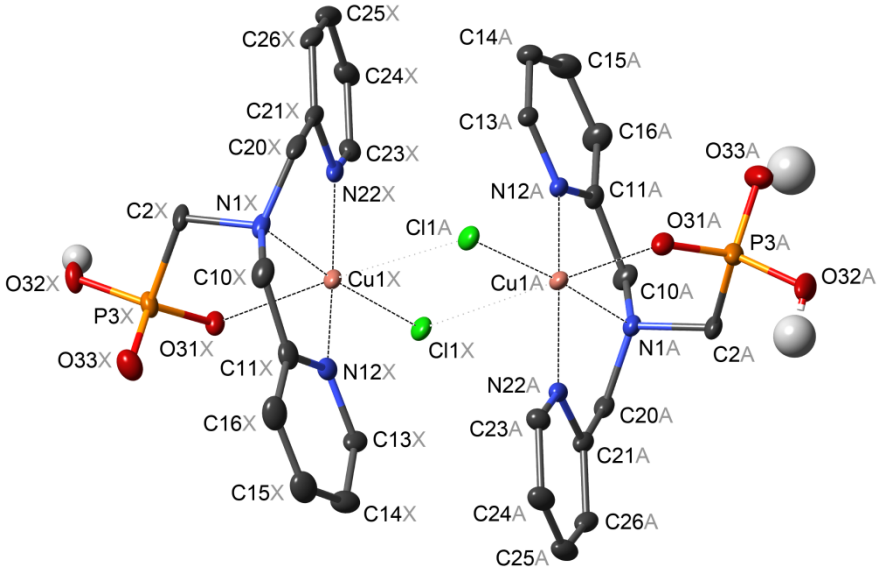

Figure S19. Crystal packing found in the crystal structure of $[CuCl(H_2\mathbf{L}^1)][CuCl(H\mathbf{L}^1)]Cl\cdot H_2O$. Water molecules of crystallization, non-coordinated chloride anions and carbon-bound hydrogen atoms are not shown.

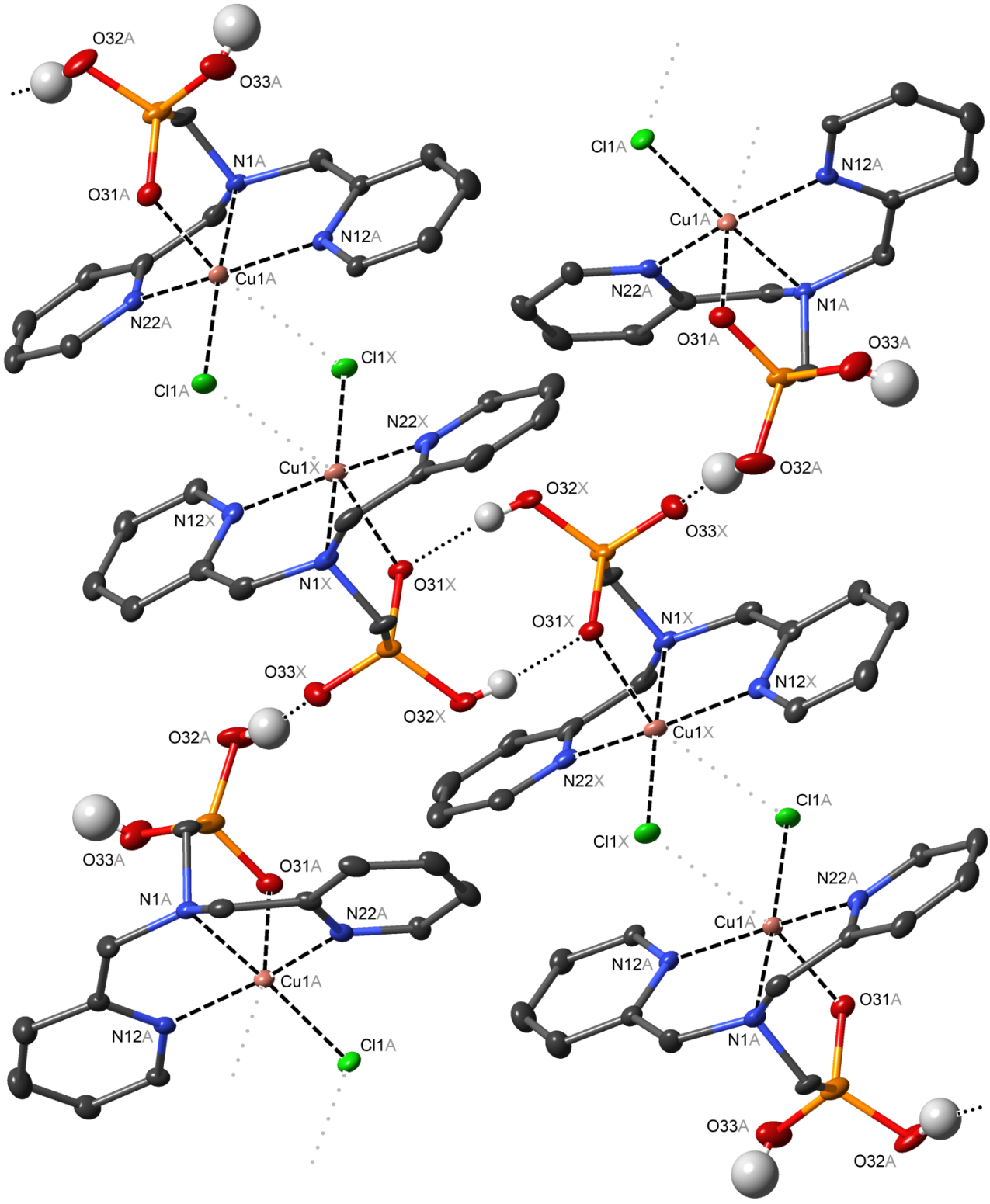

Figure S20. [Ni(H_2O)(NCS)(H**L**^{4})] unit found in crystal structure of [Ni(H_2O)(NCS)(H**L**^{4})]·H_2O. Carbon-bound hydrogen atoms are not shown.

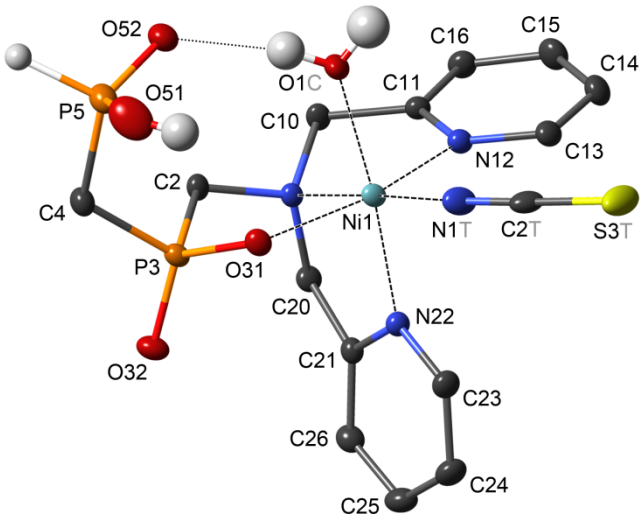

Figure S21. Bottom-to-bottom dimer {Li(H_2O)$_2$[Cu(Cl)(**L**^{4})]}$_2$ found in the crystal structure of {Li(H_2O)$_2$[Cu(Cl)(**L**^{4})]}·3H_2O.

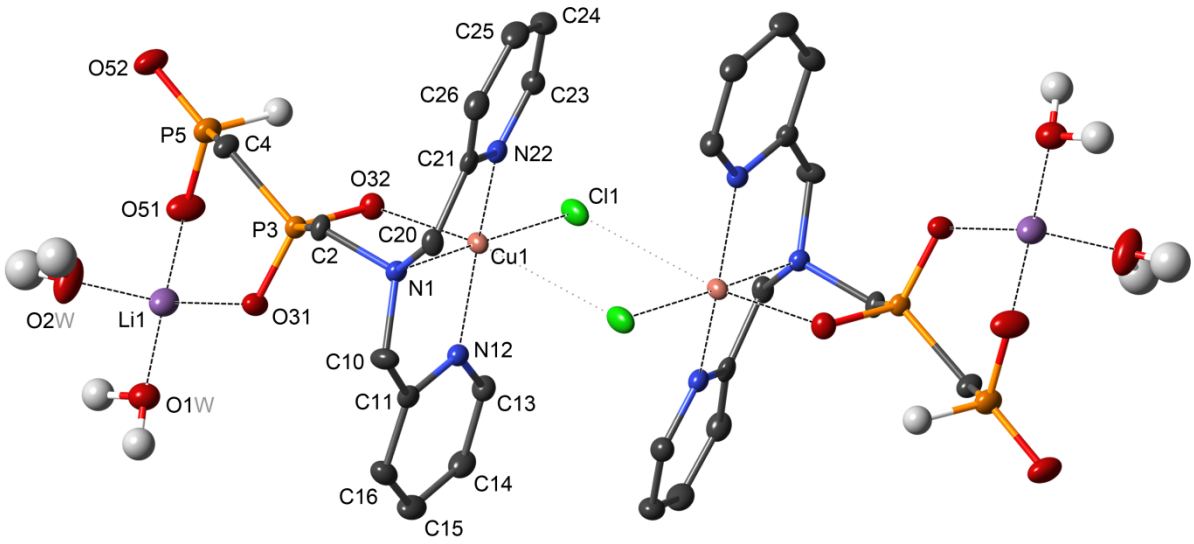

Table S5. Geometries of Ni(II) coordination spheres found in the crystal structure of $Li\{Li(H_2O)_3[LiNi_2(OH)_2(\mathbf{L^1})_2]\}(ClO_4)\cdot 11H_2O$.

distances (Å)	molecule A	molekule X	angles (°)	molecule A	molecule X
Ni1–N1	2.145(2)	2.112(2)	N1–Ni1–N12	79.48(7)	80.35(7)
Ni1–N12	2.086(2)	2.071(2)	N1–Ni1–N22	81.77(7)	81.85(7)
Ni1–N22	2.064(2)	2.093(2)	N1–Ni1–O31	84.77(6)	86.88(6)
Ni1–O31	2.180(2)	2.113(2)	N1–Ni1–O1W	100.27(6)	174.24(6)
Ni1–O1W	2.058(2)	2.033(1)	N1–Ni1–O2W	176.95(7)	96.78(6)
Ni1–O2W	2.051(2)	2.086(3)	N12–Ni1–N22	90.54(7)	92.44(7)
			N12–Ni1–O31	163.64(6)	167.03(6)
			N12–Ni1–O1W	95.25(6)	105.29(6)
			N12–Ni1–O2W	98.72(7)	91.58(7)
			N22–Ni1–O31	91.57(7)	87.97(6)
			N22–Ni1–O1W	174.13(7)	98.87(6)
			N22–Ni1–O2W	95.82(7)	175.47(7)
			O31–Ni1–O1W	83.16(6)	87.44(6)
			O31–Ni1–O2W	97.20(6)	87.64(6)
			O1W–Ni1–O2W	82.31(6)	82.06(6)

Table S6. Geometries of Cu(II) coordination spheres found in the crystal structures of studied copper(II) complexes.

	[Cu(Cl)(H**L**^{1})]·3H_2O	[Cu(Cl)(H**L**^{1})]	[Cu(Cl)(H_2**L**^{1})][Cu(Cl)(H**L**^{1})]Cl·H_2O		Na[Cu(Cl)(**L**^{4})]·0.8H_2O	{Li(H_2O)$_2$[Cu(Cl)(**L**^{4})]}·3H_2O
			[Cu(Cl)(H_2**L**^{1})] unit	[Cu(Cl)(H**L**^{1})] unit		
distances (Å)						
Cu1–N1	2.086(2)	2.072(2)	2.076(3)	2.052(3)	2.077(3)	2.085(1)
Cu1–N12	1.993(2)	2.001(2)	1.992(4)	1.989(4)	1.995(3)	2.008(1)
Cu1–N22	1.994(2)	2.008(2)	1.995(4)	1.995(4)	1.994(3)	2.007(1)
Cu1–O31	2.269(2)	2.191(2)[#b]	2.218(3)	2.387(3)	2.351(3)	2.261(1)
Cu1–Cl1	2.2597(6)	2.2586(6)	2.265(1)	2.245(1)	2.2669(8)	2.2719(4)
Cu1–Cl1[#]	3.3735(7)[a]	–	3.369(1)[c]	3.373(1)[d]	3.193(1)[a]	3.2875(5)[e]
angles (°)						
N1–Cu1–N12	83.03(7)	81.29(8)	83.0(1)	83.9(2)	82.9(1)	83.22(5)
N1–Cu1–N22	80.96(7)	81.18(8)	81.2(2)	81.4(2)	81.3(1)	80.83(5)
N1–Cu1–O31	85.70(6)	89.34(8)[#b]	89.3(1)	85.5(1)	87.4(1)	86.11(5)
N1–Cu1–Cl1	175.83(5)	159.81(6)	174.0(1)	173.6(1)	175.26(8)	175.24(4)
N12–Cu1–N22	157.76(8)	161.34(9)	159.9(2)	162.6(2)	161.1(1)	158.74(6)
N12–Cu1–O31	92.24(7)	91.11(8)[#b]	94.9(1)	89.4(1)	91.3(1)	88.00(5)
N12–Cu1–Cl1	98.53(6)	97.90(6)	97.7(1)	98.0(1)	97.89(8)	98.19(4)
N22–Cu1–O31	101.82(7)	95.03(8)[#b]	97.3(1)	98.6(1)	98.2(1)	104.78(5)
N22–Cu1–Cl1	96.47(6)	96.35(6)	96.7(1)	95.7(1)	97.04(8)	96.65(4)
O31–Cu1–Cl1	98.08(4)	110.85(5)[#b]	96.65(9)	100.65(8)	97.24(6)	98.47(3)

[#] Atom belonging to neighbouring molecule. [a] Symmetry-related atom, –*x*+1, –*y*+1, –*z*. [b] Symmetry-related atom, *x*+1/2, –*y*+3/2, *z*+1/2. [c] Atom belonging to neighbouring [Cu(Cl)(H**L**^{1})] unit, –*x*+1, –*y*+1/2, –*z*+1/2. [d] Atom belonging to neighbouring [Cu(Cl)(H_2**L**^{1})] unit, –*x*+1, *y*–1/2, –*z*+1/2. [e] Symmetry-related atom, –*x*+1, –*y*+1, –*z*+1

Table S7. Coordination geometry of Ni(II) ions found in the crystal structures of {[Ni(NCS)(**L**^{3})]$_2$}·*i*-PrOH and [Ni(H$_2$O)(NCS)(H**L**^{4})]·H$_2$O.

distances (Å)	{[Ni(NCS)(**L**^{3})]$_2$}·*i*-PrOH	[Ni(H$_2$O)(NCS)(H**L**^{4})]·H$_2$O	angles (°)	{[Ni(NCS)(**L**^{3})]$_2$}·*i*-PrOH	[Ni(H$_2$O)(NCS)(H**L**^{4})]·H$_2$O	angles (°)	{[Ni(NCS)(**L**^{3})]$_2$}·*i*-PrOH	[Ni(H$_2$O)(NCS)(H**L**^{4})]·H$_2$O
Ni1–N1	2.142(2)	2.113(1)	N1–Ni1–N12	78.52(6)	79.13(5)	N12–Ni1–O32$^{\#}$/O1C^{a}	86.32(5)	88.21(5)
Ni1–N12	2.079(2)	2.094(1)	N1–Ni1–N22	81.07(6)	83.17(5)	N12–Ni1–N1T	95.31(6)	98.39(5)
Ni1–N22	2.100(2)	2.048(1)	N1–Ni1–O31	87.17(5)	85.66(4)	N22–Ni1–O31	86.09(6)	88.16(4)
Ni1–O31	2.070(1)	2.162(1)	N1–Ni1–O32$^{\#}$/O1C^{a}	95.63(6)	91.83(5)	N22–Ni1–O32$^{\#}$/O1C^{a}	175.79(6)	174.04(5)
Ni1–O32$^{\#}$/O1C^{a}	2.075(1)	2.071(1)	N1–Ni1–N1T	170.10(6)	175.65(5)	N22–Ni1–N1T	91.94(7)	93.48(5)
Ni1–N1T	2.025(2)	2.021(1)	N12–Ni1–N22	95.53(6)	94.01(5)	O31–Ni1–O32$^{\#}$/O1C^{a}	91.16(5)	88.23(5)
			N12–Ni1–O31	165.14(6)	164.25(4)	O31–Ni1–N1T	99.40(6)	97.04(5)
						O32$^{\#}$/O1C^{a}–Ni1–N1T	91.66(6)	91.66(5)

$^{\#}$ Symmetry-related atom (–*x*, –*y*+1, –*z*+1, valid for the case of {[Ni(NCS)(**L**^{3})]$_2$}·*i*-PrOH). ^{a} Coordinated water molecule (valid for the case of [Ni(H$_2$O)(NCS)(H**L**^{4})]·H$_2$O).

Table S8. Coordination geometries of studied ligands, DPA and H**BPG** in Cu(II) complexes.

Ligand	H_2**L**^{1} [a]	H_2**L**^{1} [b]	H_2**L**^{1} [c]	H_2**L**^{1} [d]	H_2**L**^{4} [e]	H_2**L**^{4} [f]
$Cu–N_{am}$ (Å)	2.086	2.072	2.076	2.052	2.077	2.085
$Cu–N_{py}$ (Å)	1.993	2.001	1.992	1.989	1.995	2.008
$Cu–N_{py}$ (Å)	1.994	2.008	1.995	1.995	1.994	2.007
$N_{py}–Cu–N_{py}$ (°)	157.8	161.3	159.9	162.6	161.1	158.7

Ligand	DPA [3]	DPA [3]	DPA [3]	DPA [4]	DPA [4]	DPA [5]
$Cu–N_{am}$ (Å)	1.995	2.030	2.029	1.998	2.066/ 1.980[g]	1.989
$Cu–N_{py}$ (Å)	2.042	2.005	2.022	1.983	1.981	1.982
$Cu–N_{py}$ (Å)	1.989	1.989	2.021	1.968	1.985	1.990
$N_{py}–Cu–N_{py}$ (°)	161.1	161.1	161.2	161.3	163.4	162.4

Ligand	H**BPG** [6]	H**BPG** [7]	H**BPG** [8]	H**BPG** [9]	H**BPG** [10]	H**BPG** [11]	H**BPG** [11]
$Cu–N_{am}$ (Å)	2.059	2.076	2.072	1.957	2.059	2.067	2.075
$Cu–N_{py}$ (Å)	1.979	1.970	2.009	1.931	1.978	1.982	1.995
$Cu–N_{py}$ (Å)	1.981	1.975	1.994	1.937	2.001	1.978	1.995
$N_{py}–Cu–N_{py}$ (°)	162.2	164.3	159.5	169.3	163.3	163.4	161.8

[a] [CuCl(H**L**^{1})]·3H_2O; [b] [CuCl(H**L**^{1})]; [c] [CuCl(H_2**L**^{1})][CuCl(H**L**^{1})]Cl·H_2O – [CuCl(H_2**L**^{1})] unit;
[d] [CuCl(H_2**L**^{1})][CuCl(H**L**^{1})]Cl·H_2O – [CuCl(H**L**^{1})] unit; [e] Na[CuCl(**L**^{4})]·0.8H_2O; [f] {Li(H_2O)$_2$[CuCl(**L**^{4})]}·3H_2O;
[g] Amino group was found to be disordered in two positions.

Table S9. Coordination geometries of studied ligands and DPA in Ni(II) complexes.

Ligand	H**L**^{3} [a]	H_2**L**^{4} [b]	DPA [5]	DPA [12]	DPA [12]	DPA [12]
Ni–N_{am} (Å)	2.142	2.113	2.071	2.105	2.076	2.078
Ni–N_{py} (Å)	2.079	2.094	2.033	2.088	2.085	2.053
Ni–N_{py} (Å)	2.100	2.048	2.050	2.062	2.051	2.099
N_{am}–Ni–N_{py} (°)	78.5	79.1	83.0	79.5	81.0	83.5
N_{am}–Ni–N_{py} (°)	81.1	83.2	82.7	82.3	82.9	80.7
N_{py}–Ni–N_{py} (°)	95.5	94.0	87.4	94.7	88.3	86.6

[a] {[Ni(NCS)(**L**^{3})]$_2$}·*i*PrOH ; [b] [Ni(H_2O)(NCS)(H**L**^{4})]·H_2O

Figure S22. Numbering of DPA fragment used in NMR characterization of H_2**L**^{1}–H_2**L**^{4}.

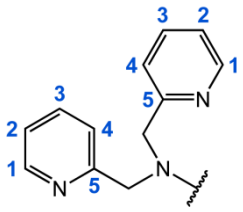

Table S10. Experimental crystallographic data of reported crystal structures.

	$(H_3\mathbf{L^1})Cl{\cdot}2H_2O$	$\{[Li(H\mathbf{L^1})]_2\}$	$Li\{Li(H_2O)_3[LiNi_2(OH)_2(\mathbf{L^1})_2]\}(ClO_4){\cdot}11H_2O$	$[Cu(Cl)(H\mathbf{L^1})]$	$[Cu(Cl)(H\mathbf{L^1})]{\cdot}3H_2O$	$[Cu(Cl)(H_2\mathbf{L^1})][Cu(Cl)(H\mathbf{L^1})]Cl{\cdot}H_2O$
	CCDC-1815210	CCDC-1815209	CCDC-1815204	CCDC-1815212	CCDC-1815206	CCDC-1815207
Formula	$C_{13}H_{21}ClN_3O_5P$	$C_{26}H_{30}Li_2N_6O_6P_2$	$C_{26}H_{58}ClLi_3N_6Ni_2O_{26}P_2$	$C_{13}H_{15}ClCuN_3O_3P$	$C_{13}H_{21}ClCuN_3O_6P$	$C_{26}H_{33}Cl_3Cu_2N_6O_7P_2$
M_r	365.75	598.38	1106.41	391.24	445.29	836.95
Colour	colourless	colourless	blue	blue	blue	blue
Shape	plate	plate	prism	prism	plate	prism
Dimensions (mm)	0.059×0.070×0.160	0.064×0.185×0.250	0.136×0.306×0.307	0.083×0.139×0.247	0.065×0.186×0.262	0.106×0.135×0.136
Crystal system	orthorhombic	monoclinic	monoclinic	monoclinic	triclinic	monoclinic
Space group	$Pna2_1$	$P2_1/n$	$P2_1/c$	$P2_1/n$	$P\bar{1}$	$P2_1/c$
a (Å)	8.6070(2)	9.3018(3)	9.3666(4)	9.2402(3)	8.0880(4)	8.3721(2)
b (Å)	25.0089(5)	9.3173(3)	35.0692(15)	13.3847(4)	8.5326(5)	22.6005(6)
c (Å)	7.6190(2)	16.7701(5)	14.1635(5)	12.0873(4)	14.6161(8)	17.3031(6)
α (°)	–	–	–		73.868(2)	–
β (°)	–	95.0570(10)	101.461(2)	104.5790(10)	74.070(2)	97.159(2)
γ (°)	–	–	–		69.458(2)	–
V (Å^3)	1640.00(7)	1447.77(8)	4559.6(3)	1446.79(8)	889.62(9)	3248.46(16)
Z	4	2	4	4	2	4
D_{calc} (g cm^{-3})	1.481	1.373	1.612	1.796	1.662	1.711
μ (mm^{-1})	3.254	1.795	1.048	1.820	1.503	1.709
F(000)	768	624	2304	796	458	1704
Unique diffractions; observed ($I > 2\sigma(I)$)	3203; 3093	2864; 2662	10490; 9453	3317; 3104	4103; 3393	7476; 5598
Parameters	236	194	696	204	251	431
G-o-f on F^2	1.085	1.236	1.035	1.114	1.055	1.050
R; R' (all data)	0.0264; 0.0278	0.0363; 0.0392	0.0372; 0.0420	0.0262; 0.0295	0.0342; 0.0449	0.0527; 0.0792
wR; wR' (all data)	0.0651; 0.0659	0.1009; 0.1023	0.0900; 0.0931	0.0809; 0.0828	0.0871; 0.0918	0.1245; 0.1379
Diff. max; min (e Å^{-3})	0.174; –0.291	0.308; –0.362	1.981; –0.750	0.401; –0.558	0.524; –0.387	1.226; –1.375

	{[Ni(NCS)(**L**^{3})]$_2$} ·*i*-PrOH CCDC-1815213	[Ni(H$_2$O)(NCS)(H**L**^{4})] ·H$_2$O CCDC-1815211	Na[Cu(Cl)(**L**^{4})] ·0.8H$_2$O CCDC-1815208	{Li(H$_2$O)$_2$[Cu(Cl)(**L**^{4})]} ·3H$_2$O CCDC-1815205
Formula	$C_{30}H_{34}N_8Ni_2O_4P_2S_2$	$C_{15}H_{22}N_4NiO_6P_2S$	$C_{14}H_{18.6}ClCuN_3NaO_{4.8}P_2$	$C_{14}H_{27}ClCuLiN_3O_9P_2$
M_r	814.13	507.07	489.64	549.25
Colour	light blue	blue	blue	light blue
Shape	plate	prism	prism	prism
Dimensions (mm)	0.035×0.104×0.194	0.064×0.132×0.233	0.055×0.120×0.132	0.070×0.203×0.301
Crystal system	monoclinic	monoclinic	triclinic	triclinic
Space group	*P*21/*c*	*C*2/*c*	*P*–1	*P*–1
a (Å)	12.4639(4)	20.2640(9)	8.4334(3)	8.2892(4)
b (Å)	10.6323(4)	13.5918(6)	8.5412(4)	8.6425(4)
c (Å)	15.2654(5)	14.8142(6)	14.2914(6)	16.9266(8)
α (°)		–	86.225(2)	80.319(2)
β (°)	102.2710(10)	90.348(2)	77.544(2)	83.468(2)
γ (°)		–	73.399(2)	67.517(2)
V (Å^3)	1976.75(12)	4080.1(3)	963.29(7)	1102.86(9)
Z	2	8	2	2
D_{calc} (g cm^{-3})	1.368	1.651	1.688	1.654
μ (mm^{-1})	1.181	1.251	1.491	1.307
F(000)	840	2096	498	566
Unique diffractions; observed ($I > 2\sigma(I)$)	3880; 3374	4696; 4296	4414; 4011	5074; 4637
Parameters	225	286	262	318
G-o-f on F^2	1.046	1.053	1.047	1.058
R; *R*' (all data)	0.0278; 0.0343	0.0229; 0.0265	0.0478; 0.0525	0.0254; 0.0295
wR; *wR*' (all data)	0.0661; 0.0683	0.0584; 0.0604	0.1274; 0.1309	0.0613; 0.0632
Diff. max; min (e Å^{-3})	0.622; –0.439	0.316; –0.469	1.868; –1.039	0.687; –0.506

Syntheses

Synthesis of H_2L^1

In a 250 mL flask, H_3PO_3 (20.6 g; 251 mmol), DPA (5.05 g; 25.3 mmol) and paraformaldehyde (837 mg; 27.9 mmol) were suspended in aqueous HCl (12 M; 100 mL) and the flask was immediately closed by a stopper. The reaction mixture was then stirred 2 d at 80 °C. After cooling to room temperature, the mixture was evaporated to dryness and twice co-evaporated with H_2O to remove HCl. The residue was purified on strong cation exchange resin (DOWEX 50; ~150 mL; H^+-form; H_2O → 10% aq. pyridine). Pyridine fraction with product was evaporated to dryness, several times co-evaporated with H_2O to remove pyridine quantitatively and then dried in vacuum to a constant weight. The residual yellow oil (pure product in zwitterionic form) was dissolved in aqueous HCl (3%, 30 mL) and transferred to a 500 ml beaker. Excess of *i*-PrOH (~ 100 mL) was then added to produce cloudiness. After standing for several days, the formed colourless crystals were filtered off, washed with *i*-PrOH, then with Et_2O and air dried. Product was obtained in the form of hydrochloride dihydrate as colourless crystals (suitable for X-ray diffraction). **Conversion** (^{31}P NMR): ~90% (2 d). **Yield:** 6.15 g of colourless hydrochloride crystals (66%; based on DPA). **NMR** (D_2O, pD ~ 5): **^{1}H** δ 3.14 (P–C*H*$_2$–N, d, 2H, $^2J_{HP}$ = 11); 4.29 (C*H*$_2$–N–C*H*$_2$, s, 4H); 7.53 (*H*$_2$, ddd, 2H, $^3J_{HH}$ = 8, $^3J_{HH}$ = 5, $^4J_{HH}$ = 1); 7.55 (*H*$_4$, ddd, 2H, $^3J_{HH}$ = 8, $^4J_{HH}$ = 1, $^5J_{HH}$ = 1); 8.02 (*H*$_3$, td, 2H, $^3J_{HH}$ = 8, $^4J_{HH}$ = 2); 8.47 (*H*$_1$, ddd, 2H, $^3J_{HH}$ = 5, $^4J_{HH}$ = 2, $^5J_{HH}$ = 1); **^{13}C**{^{1}H} δ 54.6 (P–CH_2–N, d, $^1J_{CP}$ = 147); 59.9 (*C*H$_2$–N–*C*H$_2$, d, $^3J_{CP}$ = 7); 125.3 (*C*$_2$, s); 126.2 (*C*$_4$, s); 142.9 (*C*$_3$, s); 145.3 (*C*$_1$, s); 154.8 (*C*$_5$, s); **^{31}P**{^{1}H} δ 17.2 (s). **ESI-MS**: **(−)** 291.9 [M−H$^+$]$^-$; **(+)** 294.1 [M+H$^+$]$^+$; 316.0 [M+Na$^+$]$^+$. **TLC** (EtOH – conc. aq. NH_4OH 3:1): R_f ~ 0.2. **HPLC**: R_f ~ 5.7 min. **EA** ($C_{13}H_{16}N_3O_3P{\cdot}HCl{\cdot}2H_2O$, M_R = 365.8): C 42.7 (42.9); H 5.8 (5.8); N 11.5 (11.4).

Synthesis of HL^2

In a 250 mL flask, H_3PO_2 (16.5 g; 250 mmol), DPA (5.07 g; 25.4 mmol) and paraformaldehyde (1.30 g; 43.3 mmol) were suspended in aqueous HCl (12 M; 100 mL) and the flask was immediately closed by stopper. The reaction mixture was then stirred at 30 °C for 1 d. After cooling to room temperature, the mixture was evaporated to dryness and twice co-evaporated with H_2O to remove HCl. The residue was purified on strong cation exchange resin (DOWEX 50; ~100 mL; H^+-form; H_2O → 10% aq. pyridine). Pyridine fraction with product was evaporated to dryness and several times co-evaporated with H_2O to remove pyridine quantitatively. The oily residue was further dried in vacuum to a constant weight. Product was obtained in zwitterionic form as a yellow oil. **Conversion** (^{31}P NMR): ~95% (1 d). **Yield**: 6.24 g (89%; based on DPA). **NMR** (D_2O, pD ~ 5): **^{1}H** δ 2.95 (P–C*H*$_2$–N, d, 2H,

$^{2}J_{HP}$ = 9); 4.11 (C*H*$_2$–N–C*H*$_2$, s, 4H); 7.00 (P*H*, d, 1H, $^{1}J_{HP}$ = 518); 7.46 (*H*$_2$, ddd, 2H, $^{3}J_{HH}$ = 8, $^{3}J_{HH}$ = 5, $^{4}J_{HH}$ = 1); 7.52 (*H*$_4$, ddd, 2H, $^{3}J_{HH}$ = 8, $^{4}J_{HH}$ = 1, $^{5}J_{HH}$ = 1); 7.96 (*H*$_3$, td, 2H, $^{3}J_{HH}$ = 8, $^{4}J_{HH}$ = 2); 8.40 (*H*$_1$, ddd, 2H, $^{3}J_{HH}$ = 5, $^{4}J_{HH}$ = 2, $^{5}J_{HH}$ = 1); **^{13}C**{^{1}H} δ 57.3 (P–*C*H$_2$–N, d, $^{1}J_{CP}$ = 102); 60.3 (*C*H$_2$–N–*C*H$_2$, d, $^{3}J_{CP}$ = 7); 125.2 (*C*$_2$, s); 126.3 (*C*$_4$, s); 142.7 (*C*$_3$, s); 145.4 (*C*$_1$, s); 155.3 (*C*$_5$, s); **^{31}P** δ 22.1 (dt, $^{1}J_{PH}$ = 518, $^{2}J_{PH}$ = 9). **ESI-MS**: **(−)** 275.9 [M−H$^+$]$^-$; **(+)** 300.1 [M+Na$^+$]$^+$. **TLC** (EtOH – conc. aq. NH$_4$OH 50:1): R_f ~ 0.5. **HPLC**: R_f ~ 6.3 min.

Synthesis of HL^3

In a 20 mL glass vial, methylphosphinic acid (1.41 g; 16.7 mmol), DPA (320 mg; 1.61 mmol) and paraformaldehyde (245 mg; 8.17 mmol) were suspended in aqueous HCl (12 M; 5 mL) and the vial was immediately closed by a stopper. The reaction mixture was then stirred at 95 °C for 2 d. After cooling to room temperature, the mixture was evaporated to dryness and twice co-evaporated with H_2O to remove HCl. The residue was purified on strong cation exchange resin (DOWEX 50; ~75 mL; H^+-form; H_2O → 10% aq. pyridine). Pyridine fraction with product was evaporated to dryness and several times co-evaporated with H_2O to remove pyridine quantitatively. The oily residue was purified by reverse-phase flash chromatography (C18). Fraction with pure product were combined and evaporated to dryness and then dried in vacuum to a constant weight. Product was obtained in zwitterionic form as slightly yellow oil. **Conversion** (^{31}P NMR): ~ 55% (2 d). **Yield**: 206 mg (44%; based on DPA). **NMR** (D_2O, pD ~ 4): **^{1}H** δ 1.32 (C*H*$_3$, d, 3H, $^{2}J_{HP}$ = 14); 3.10 (P–C*H*$_2$–N, d, 2H, $^{2}J_{HP}$ = 7); 4.35 (*C*H$_2$–N–*C*H$_2$, s, 4H); 7.72–7.82 (*H*$_8$+*H*$_{10}$, m, 4H); 8.28 (*H*$_3$, td, 2H, $^{3}J_{HH}$ = 8, $^{4}J_{HH}$ = 1); 8.63 (*H*$_1$, dm, 2H, $^{3}J_{HH}$ = 6); **^{13}C**{^{1}H} δ 15.1 (*C*H$_3$, d, $^{1}J_{CP}$ = 93); 56.0 (P–*C*H$_2$–N, d, $^{1}J_{CP}$ = 103); 58.6 (*C*H$_2$–N–*C*H$_2$, d, $^{3}J_{CP}$ = 6); 125.4 (*C*$_2$, s); 126.3 (*C*$_4$, s); 143.0 (*C*$_1$, s); 144.6 (*C*$_3$, s); 153.6 (*C*$_5$, s); **^{31}P**{^{1}H} δ 43.6 (s). **ESI-MS**: **(−)** 290.1 [M−H$^+$]$^-$; **(+)** 292.3 [M+H$^+$]$^+$; 314.3 [M+Na$^+$]$^+$. **TLC** (EtOH – conc. aq. NH$_4$OH 50:1): R_f ~ 0.3. **HPLC**: R_f ~ 7.4 min.

Synthesis of H_2L^4

In a 250 mL glass flask, methylene-bis(phosphinic acid) (4.10 g; 28.5 mmol) and DPA (1.10 g; 5.52 mmol) were dissolved in aqueous HCl (12 M; 30 mL). Paraformaldehyde (173 mg; 5.77 mmol) was then added and the flask was immediately closed by stopper. The reaction mixture was stirred at 50 °C for 1 d. After cooling to room temperature, the mixture was evaporated to dryness and twice co-evaporated with H_2O to remove HCl. The residue was purified on strong cation exchange resin (DOWEX 50; ~100 mL; H^+-form; H_2O → 10% aq. pyridine). Pyridine fraction with product was evaporated to dryness and several times co-

evaporated with H_2O to remove pyridine quantitatively. The residual yellow oil was dissolved in minimal amounts of EtOH and purified by column chromatography (SiO_2; ~150 g; EtOH – conc. aq. NH_4OH 10:1). Fractions with pure product were combined and evaporated to dryness, and then several times with H_2O to remove ammonia. The residue was dissolved in H_2O (~50 mL) and purified on strong cation exchange resin (DOWEX 50; ~150 mL; H^+-form; H_2O → 10% aq. pyridine). Pyridine fraction with product was evaporated to dryness and several times co-evaporated with H_2O to remove pyridine quantitatively. The resulting oil was further dried in vacuum to constant weight. Product was obtained in zwitterionic form as a yellow oil. **Conversion** (^{31}P NMR): ~85% (1 d). **Yield:** 1.03 g (53%; based on DPA). **NMR** (D_2O, pD ~ 3): **^{1}H** δ 2.23 (P–C*H*$_2$–P, td, 2H, $^2J_{HP}$ = 17, $^3J_{HH}$ = 2); 3.14 (P–C*H*$_2$–N, d, 2H, $^2J_{HP}$ = 10); 4.41 (C*H*$_2$–N–C*H*$_2$, s, 4H); 7.28 (P*H*, ddt, 1H, $^1J_{HP}$ = 541, $^3J_{HP}$ = 4, $^3J_{HH}$ = 2); 7.80–7.84 (*H*$_4$, m, 2H); 7.82–7.87 (*H*$_2$, m, 2H); 8.40 (*H*$_3$, td, 2H, $^3J_{HH}$ = 8, $^4J_{HH}$ = 1); 8.70 (*H*$_1$, ddd, 2H, $^3J_{HH}$ = 6, $^4J_{HH}$ = 2, $^5J_{HH}$ = 1); **^{13}C**{^{1}H} δ 39.1 (P–*C*H$_2$–P, t, $^1J_{CP}$ = 78); 54.6 (P–*C*H$_2$–N, d, $^1J_{CP}$ = 111); 58.8 (*C*H$_2$–N–*C*H$_2$, d, $^3J_{CP}$ = 7); 126.7 (*C*$_2$, s); 127.4 (*C*$_4$, s); 142.0 (*C*$_1$, s); 147.2 (*C*$_3$, s); 153.5 (*C*$_5$, s); **^{31}P** δ 20.6 (*P*H, dtd, 1P, $^1J_{PH}$ = 541, $^2J_{PH}$ = 17, $^2J_{PP}$ = 6); 29.6 (CH$_2$–*P*–CH$_2$, m, 1P). **ESI-MS**: **(−)** 354.1 [M−H$^+$]$^-$; **(+)** 355.7 [M+H$^+$]$^+$; 378.2 [M+Na$^+$]$^+$; 394.1 [M+K$^+$]$^+$. **TLC** (EtOH – conc. aq. NH_4OH 10:1): R_f ~ 0.3. **HPLC**: R_f ~ 3.4 min.

Preparation of single crystals

{[Li(HL^1)]$_2$}

Solid H_2**L^1**·HCl·2H_2O (102.6 mg; 280 µmol) and solid LiOH·H_2O (24.0 mg; 572 µmol) were dissolved in deionized H_2O (500 µL), followed by addition of *i*-PrOH (~15 mL). The mixture was briefly shaken and the resulting clear solution was left standing at room temperature. After several days, colourless crystals were formed.

Li{Li(H$_2$O)$_3$[LiNi$_2$(OH)$_2$(L^1)$_2$]}(ClO$_4$)·11H$_2$O

Solid H_2**L^1**·HCl·2H_2O (99.3 mg; 271 µmol), solid $NiCl_2$·6H_2O (64.5 mg; 271 µmol), $LiClO_4$·3H_2O (22.2 mg; 138 µmol) and LiOH·H_2O (45.7 mg; 1.09 mmol) were dissolved in deionized H_2O (500 µL) and the mixture was briefly shaken. Then, *i*-PrOH (~15 mL) was carefully added to overlayer the aq. solution and the closed vial was left standing at room temperature. After several days, grey-blue crystals were formed.

[Cu(Cl)(HL^1)]·3H$_2$O

Solid H_2**L^1**·HCl·2H_2O (99.8 mg; 273 µmol) and solid $CuCl_2$·2H_2O (50.9 mg; 292 µmol) were dissolved in H_2O (500 µL), followed by addition of solid LiOH·H_2O (26.7 mg; 636

μmol). The mixture was briefly shaken. Then, *i*-PrOH (~15 mL) was carefully added to overlayer the aq. solution and the closed vial was left standing at room temperature. After several days, light blue crystals were formed.

[Cu(Cl)(HL^{1})]

Long standing (several months) of [Cu(Cl)(H**L**^{1})]·3H_2O crystals prepared as above under the mother liquour led to formation of dark green crystals of [Cu(Cl)(H**L**^{1})].

[Cu(Cl)(H_2L^{1})][Cu(Cl)(HL^{1})]Cl·H_2O

Solid H_2**L**^{1}·HCl·2H_2O (97.3 mg; 266 μmol) and solid $CuCl_2$·2H_2O (47.4 mg; 278 μmol) were dissolved in H_2O (500 μL), followed by addition of solid LiOH·H_2O (23.9 mg; 569 μmol). The mixture was briefly shaken. Slow diffusion of *i*-PrOH vapours then yielded light blue crystals.

{[Ni(NCS)(L^{3})]$_2$}·*i*-PrOH

Aq. solution of freshly prepared H**L**^{3} (0.77 M; 367 μL; 283 μmol) was added to solution of $Ni(NCS)_2$ (49.1 mg; 281 μmol) in H_2O (450 μL) and the resulting solution was shaken. Then, *i*-PrOH (~15 mL) was carefully added to overlayer the aq. solution and the closed vial was left standing at room temperature. After several days, blue green crystals were formed.

[Ni(H_2O)(NCS)(HL^{4})]·H_2O

Aqueous solution of H_2**L**^{4} (1.0 M; 140 μL; 140 μmol) was added to solution of $Ni(NCS)_2$ (25 mg; 143 μmol) in H_2O (350 μL) and the resulting solution was shaken. Slow diffusion of *i*-PrOH vapours then yielded blue green crystals.

Na[Cu(Cl)(L^{4})]·0.8H_2O

Aqueous solution of H_2**L**^{4} (1.0 M; 88 μL; 88 μmol) was added to a solid $CuCl_2$·2H_2O (15.9 mg; 89.0 μmol) followed by addition of aqueous solution of NaOH (1.0 M; 97 μL; 97 μmol) and the resulting solution was shaken. Slow diffusion of *i*-PrOH vapours yielded light blue crystals.

{Li(H_2O)$_2$[Cu(Cl)(L^{4})]}·3H_2O

Aqueous solution of H_2**L**^{4} (1.0 M; 88 μL; 88 μmol) was added to a solid $Cu(Cl)_2$·2H_2O (15.0 mg; 88.0 μmol) followed by addition of aqueous solution of LiOH (1.0 M; 97 μL; 97 μmol) and the resulting solution was shaken. Slow diffusion of *i*-PrOH vapours yielded light blue crystals.

X-ray data acquisition and evaluation

The diffraction data were collected at 150 K (Cryostream Cooler, Oxford Cryosystem) by Nonius KappaCCD diffractometer equipped with Bruker APEX-II CCD detector using monochromatized Mo-Kα radiation (λ = 0.71073 Å, [Cu(Cl)(H**L**^{1})]·3H_2O), or with Bruker D8 VENTURE Kappa Duo PHOTON100 diffractometer with IμS micro-focus sealed tube using Cu-Kα (λ = 1.54178 Å, (H_3**L**^{1})Cl·2H_2O and {[Li(H**L**^{1})]$_2$}) or Mo-Kα (λ = 0.71073 Å, all other structures). Data were analysed using the SAINT V8.27B (Bruker AXS Inc., 2012) software package. Data were corrected for absorption effects using the multi-scan method (SADABS). All structures were solved by direct methods (SHELXS97)[13] and refined using full-matrix least-squares techniques (SHELXL2014).[14] In general, all non-hydrogen atoms were refined anisotropically except the disordered parts of the molecules with low occupancy, which were refined in isotropic regime. Most hydrogen atoms could be found in the difference density map, and the appropriate number of hydrogens bound to carbon atoms were fixed in theoretical (C–H) positions. Conversely, oxygen-bound hydrogen atoms were fully refined or DFIX command was used to maintain realistic O–H bond distances. The experimental data of the reported crystal structures are outlined in Table S7. In some of the structures, peaks higher than 1 e Å^{-3} were found close to disordered counter-ions or water molecules of crystallization, albeit with no effect on the correctness of the structure of the complexes. In the structures of (H_3**L**^{1})Cl·2H_2O, {[Li(H**L**^{1})]$_2$}, [Cu(Cl)(H**L**^{1})] and [Ni(H_2O)(NCS)(H**L**^{4})]·H_2O, no disorder was found. All hydrogen atoms were localized in difference density maps, and those bound to oxygen atoms were fully refined. In the structure of Li{Li(H_2O)$_3$[LiNi_2(OH)$_2$(**L**^{1})$_2$]}(ClO_4)·11H_2O, pseudo-cubane complex, one lithium atom and some water molecules were identified without any sign of its disorder. The perchlorate ion was found to be disordered in two positions, sharing chlorine atom and one of oxygen atoms. Remaining three oxygen atoms were refined in two staggered positions, and their relative occupancies were refined employing EADP command to 86:14%. Some hydrogen atoms of water molecules of crystallization were fully refined, and those giving unrealistic bond lengths were fixed using DFIX or AFIX commands. Identity of bridging OH groups was unambiguously confirmed – one OH group (O1W, Figure 9) is connecting LiNi_2 in μ_3 mode, allowing no space for potential binding of other hydrogen atom to form a water molecule. However, in the case of the second OH bridge (O2W, Figure 9) which connects Ni_2 in μ_2-mode, there is some free space in tetrahedral direction from the oxygen atom and one can suggest that the second hydrogen atom is bound there resulting in H_2O molecule. However, in this fourth direction (for binding of the second hydrogen atom), a water molecule of crystallization is present. Its hydrogen atom (found in difference density map) points to the hydroxido bridge, which serves as an acceptor of medium-strong hydrogen bond and, therefore, O2W atom could not belong to a water molecule. In total, all well-defined molecules

have negative charge –1. Missing positive counter-ion was best modelled as disordered lithium(I) ion in fluid channel formed by several disordered water molecules; for these molecules, appropriate hydrogen atoms could not be found. In the structures of [Cu(Cl)(H$\mathbf{L}^{\mathbf{1}}$)]·3H_2O and {Li(H_2O)$_2$[Cu(Cl)($\mathbf{L}^{\mathbf{4}}$)]}·3H_2O, no disorder was found, and all hydrogen atoms were localized in difference density maps. However, some of those bound in water molecules had to be fixed using DFIX command due to unrealistic bond lengths after their full refinement. In the structure of [Cu(Cl)($H_2\mathbf{L}^{\mathbf{1}}$)][Cu(Cl)(H$\mathbf{L}^{\mathbf{1}}$)]Cl·$H_2O$, water molecule of crystallization was found to be disordered in two close positions whose occupancies were refined employing EADP command to 69:31%. Appropriate hydrogen atoms were localized in difference density map and fixed in original positions using AFIX command. In the structure of {[Ni(NCS)($\mathbf{L}^{\mathbf{3}}$)]$_2$}·*i*PrOH, coordinated isothiocyanato ligand was slightly disordered. The disorder was modelled by splitting the CS group in two positions (74:26%). Further disorder was found for *i*PrOH molecule present close to the symmetry centre. This disorder could not be satisfactorily modelled and, therefore, appropriate electronic maxima were squeezed using PLATON.[15] In the structure of Na[Cu(Cl)($\mathbf{L}^{\mathbf{4}}$)]·0.8H_2O, distant phosphinate group was best modelled disordered in two positions (56:44%). However, negative charge of the complex molecule had to be compensated by some cation. Electronic maxima present in difference density map close to the symmetry centre were best interpreted as disordered sodium(I) ion and partially occupied disordered water molecule of crystallization. Data for the structures have been deposited the Cambridge Crystallographic Data Centre with CCDC 1815204-1815213 reference numbers (Table S6).

References

[1] Martell, A. E. and Smith, R. M. *Critical Stability Constants*; Plenum Press: New York, 1974–1989, vol. 1–6; NIST Standard Reference Database 46 (Critically Selected Stability Constants of Metal Complexes), version 5.0, 1994.

[2] K. Popov, H. Rönkkömäki and L. H. J. Lajunen *Pure Appl. Chem.* 2001, **73**, 1641.

[3] C.-M. Liu, S. Gao, H.-Z. Kou, D.-Q. Zhang, H.-L. Sun and D.-B. Zhu, *Cryst. Growth Des.*, 2006, **6**, 94.

[4] R. J. Butcher, Y. Gultneh and Allwar, *Acta Crystallogr.*, 2005, **E61**, m818.

[5] S. Rarig and J. Zubieta, *J. Solid. State Chem.*, 2002, **167**, 370.

[6] M. Bartholomä, B. Ploier, H. Cheung, W. Ouellette and J. Zubieta, *Inorg. Chim. Acta*, 2010, **363**, 1659.

[7] A. Nielsen, Ch. J. McKenzie and A. D. Bond, *Acta Crystallogr.*, 2006, **E62**, m2453.

[8] K.-Y. Choi, S.-Y. Park and A.-. Shin, *J. Chem. Crystallogr.*, 2006, **36**, 7.

[9] Y.-Ch. Cui, G.-B. Che, Ch.-B. Liu and Ch.-B. Li, *Acta Crystallogr.*, 2005, **E61**, m2355.

[10] K.-Y. Choi, Y.-M. Jeon, H. Ryu, J.-J. Oh, H.-H. Lim and M.-W. Kim, *Polyhedron*, 2004, **23**, 903.

[11] T. Okuno, S. Ohba and Y. Nishida, *Polyhedron*, 1997, **16**, 3765.

[12] A. M. Atria, M. T. Garland and R. Baggio, *Acta Crystallogr.*, 2014, **C70**, 541.

[13] Sheldrick, G. M. SHELXS97. Program for Crystal Structure Solution from Diffraction Data. University of Göttingen, Göttingen, 1997; Sheldrick, G. M. *Acta Crystallogr.*, 2008, **A64**, 112.

[14] Sheldrick, G. M. SHELXL-2014/7. Program for Crystal Structure Refinement from Diffraction Data. University of Göttingen: Göttingen, 2014.

[15] A. L. Spek, PLATON, A Multipurpose Crystallographic Tool, Utrecht University, Utrecht, 2005.